

**Susceptibility of Glass-
Reinforced Epoxy
Laminates to
Conductive Anodic
Filamentation**

**Alan Brewin, Ling Zou
& Christopher Hunt**

January 2004

Susceptibility of Glass-Reinforced Epoxy Laminate to Conductive Anodic Filamentation

Alan Brewin, Ling Zou & Christopher Hunt
Materials Centre
National Physical Laboratory
Teddington, Middlesex
UK. TW11 0LW

ABSTRACT

Conductive Anodic Filamentation (CAF) is a subsurface failure mode for woven glass-reinforced laminate (FR4) materials, in which a copper salt filament grows and results in a consequential electrical short between plated through-hole (PTH) walls or adjacent copper planes. In this study FR4 laminates, in the form of high PTH density multi-layer test circuits, were exposed to different manufacturing conditions and studied for resistance to CAF initiation and growth. CAF performance was assessed using high temperature and humidity conditions to promote failures, with a voltage applied across adjacent vias. By application of a range of voltages and via geometries the basis for a performance map for laminates was obtained for use in materials comparison. The changes due to exposure of laminates to lead-free temperatures and other processing steps were then examined using the technique, and a number of important recommendations made regarding minimising the possibility of CAF initiation and growth.

© Crown copyright 2004
Reproduced by permission of the Controller of HMSO

ISSN 1473 2734

National Physical Laboratory
Teddington, Middlesex, UK, TW11 0LW

Extracts from this report may be reproduced provided the source is
acknowledged and the extract is not taken out of context.

Approved on behalf of Managing Director, NPL, by Dr C Lea,
Head, Materials Centre

CONTENTS

1	INTRODUCTION	1
2	THE CAF MECHANISM.....	2
3	EXPERIMENTAL	6
3.1	Phase 1.....	6
3.1.1	Test vehicle design.....	6
3.1.2	Pre-conditioning of the samples.....	9
3.1.3	Artificial ageing and resistance monitoring.....	10
3.2	Locating, sectioning & analysing CAF	11
3.3	Phase 2.....	13
3.3.1	Laminate supplier	14
3.3.2	Board house	14
3.3.3	Glass transition temperature (T _g).....	15
3.3.4	CAF resistance.....	15
3.3.5	Weave	15
3.3.6	Board finish.....	15
3.3.7	Reflow	16
3.3.8	Test vehicle design - TB38B	16
3.3.9	Pre-conditioning of the samples.....	17
3.3.10	Artificial ageing and IR monitoring	17
4	RESULTS AND DISCUSSION.....	18
4.1	Phase 1.....	18
4.1.1	Trends in time to failure	18
4.1.2	Insulation resistance.....	21
4.1.3	Summary of Phase 1, and influences on Phase 2.....	25
4.1.4	Normalisation to voltage gradient	25
4.1.5	Real-time plots	26
4.1.6	Correlation of Phase 1 data to Sun/CALCE Models	27
4.2	Phase 2.....	29
4.2.1	Normalisation of data for trend analysis	29
4.2.2	Via geometry effects.....	29
4.2.3	Process and material effects	32
5	DISCUSSION	40
6	CONCLUSIONS	43
7	REFERENCES	45
8	ACKNOWLEDGEMENTS	46
9	APPENDIX A – GERBER PLOTS FOR TB38A.....	47
10	APPENDIX B – GERBER PLOTS FOR TB38B.....	49

1 INTRODUCTION

Conductive Anodic Filamentation (CAF) is a failure phenomenon seen within the bulk of glass-reinforced epoxy printed circuit board laminate, used for the manufacture of circuit assemblies. This distinct electromigration failure mode was first reported in 1979 [1, 7-15], however more recently there has been an increased concern with reliability due to CAF failure.

There are three main drivers for this concern:

- The drive to increased circuit density with smaller printed wiring board (PWB) geometries and increased layer counts in multi-layer boards
- The rapid increase of the use of electronics in harsh environments and for high reliability and safety critical applications (automotive, avionics, medical, military)
- The impending implementation of lead-free soldering processing before July 2006, which may effect laminate stability and materials choices

The combination of these factors has increased the focus on the CAF phenomenon, and now standards bodies are considering test methods to differentiate the CAF performances of PWBs.

The mechanism proposed for CAF growth is based on an electrochemical transfer of copper ions and the deposition of copper salts that are influenced by electric field, ion concentration and pH gradients. The conductive path is therefore the growth on the anode of a salt, as compared to dendritic growth on the surface of the board, which comprises metal ions depositing on the cathode. The CAF mechanism is discussed more fully in Section 2.

To date CAF has been associated primarily with mechanically drilled holes as opposed to those prepared by laser drilling. Hence, CAF is associated with through holes, where mechanical drilling disrupts the bundles of glass reinforced fibres and permits the subsequent ingress of the copper plating solution. With laser drilling this mechanical damage doesn't occur, and the same plating ingress is not expected.

In this study a range of materials, board layout configurations, thermal events, and processing steps were investigated, and a robust test method for the assessment of CAF susceptibility for laminates defined. Furthermore the data for CAF avoidance form the basis of guidelines for design and material choices.

The study was configured in two distinct phases of experimental work. The first phase was aimed at understanding the effects on CAF resistance of through-hole geometries, voltage levels, and thermal effects such as thermal cycling and lead-free reflow on a typical FR4 laminate. With this understanding Phase 2 incorporated improvements of the test vehicle design, and comparison of different laminates types, glass reinforcements, drill feed speeds and other laminate manufacturing variables. This report relates to both phases, since the choices made in Phase 2 were dependent on Phase 1 data.

This work was carried out in partnership with DTI and industry. The industrial partners came from different parts of the supply chain: Isola and Polyclad supplied laminates to the project, whilst Prestwick Circuits, Graphic Plc, and Invotec built PCBs. Users were also involved in the form of Alcatel Submarines Networks and TRW Automotive. Concoat Systems, an instrument company, helped with the analysis equipment.

2 THE CAF MECHANISM

The steps that take place in the formation of a CAF are described below.

Initiation

For CAF to occur there must be a source of copper, a electrical bias and a glass reinforcement fibre in the same locality. In dense multi-layer PCBs this can often occur at the PTH wall where the plating has ingressed into the glass bundle, although fibres protruding through the surfaces of PCBs to the locality of surface tracks have also been reported [2].

Separation of glass and epoxy

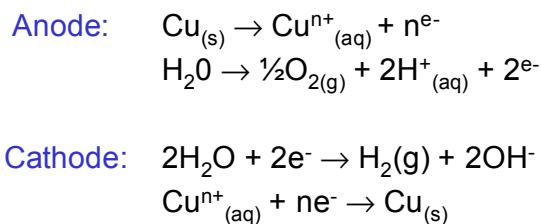
In order to facilitate good wetting of the epoxy resin into the glass fibre weave during manufacture the glass surfaces are prepared prior to impregnation. If this preparation is of poor quality, separation of the epoxy resin and glass fibres can be more likely. Bonding can also be lost due to hydrolysis of the glass finish, or even due to residual stress relief in the glass fabric weave [1], and hollow glass fibres themselves can become CAF growth routes [13].

The absorption of moisture into the laminate accelerates these processes and the delamination can then provide a pathway for CAF growth.

Electrochemical reaction

With moisture present an electrolyte can form and a pathway established for current flow that allows an electrochemical process with bias applied on the PCB. The mechanism involves oxidation and dissolution of copper at the anode, and if copper anions reach the cathode they are reduced back to copper metal (Equation 1).

Equation 1. Electrochemical equation for CAF formation



The process shown here is ideal, in reality it is solubility dependent. The formation of copper at the cathode doesn't readily happen since the copper deposits as an insoluble salt due to high pH. This solubility effect is responsible for the CAF deposits growing from the anode, a low pH environment towards the cathode, and is illustrated in Figure 1.

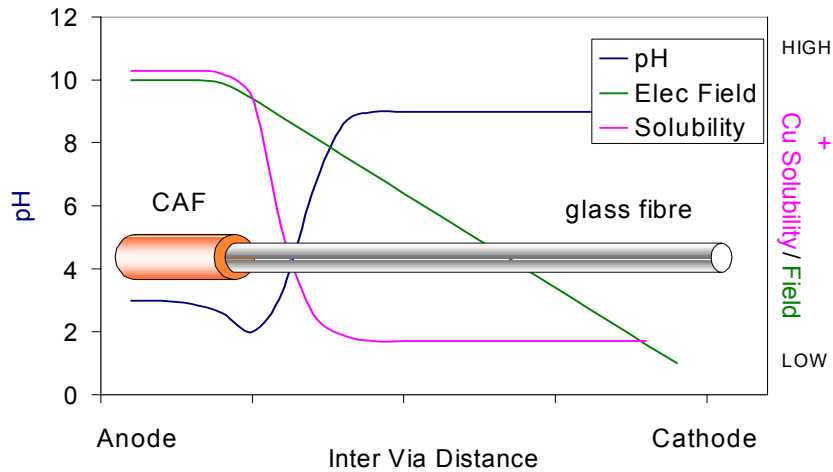


Figure 1. Schematic of pH, and electric field conditions during CAF growth.

Other ions present from processing, or materials, such as chloride, sulphide or other metals may also take part in this process.

Salt deposition

As the electrochemical dissolution of copper continues, a pH gradient is produced due to the hydroxonium ions produced at the anode and hydroxide ions at the cathode. In Figure 2 this is represented by a schematic of two through-hole vias, where the anode via wall is the initiation site.

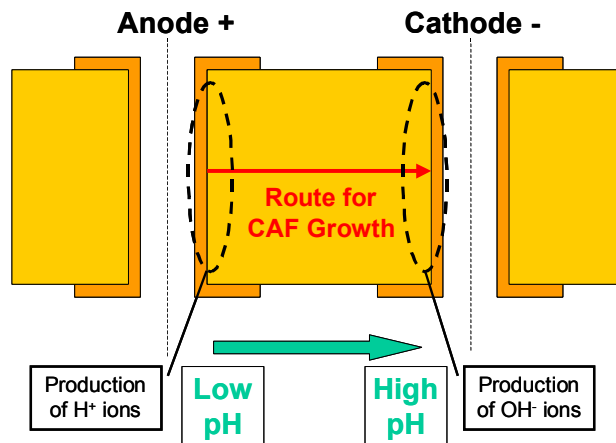


Figure 2. Schematic of CAF growth between two vias

The formation of this pH gradient is key to the mechanism of CAF growth. The solubility of copper salts is dependent on pH and the electrical potential applied, as shown by a simplified Pourbaix diagram (Figure 3). At the cathode copper metal remains stable (green area, negative potential). However at the anode, a positive potential environment with an acidic pH, the copper is mobile in solution as copper cations Cu^{2+} (blue region).

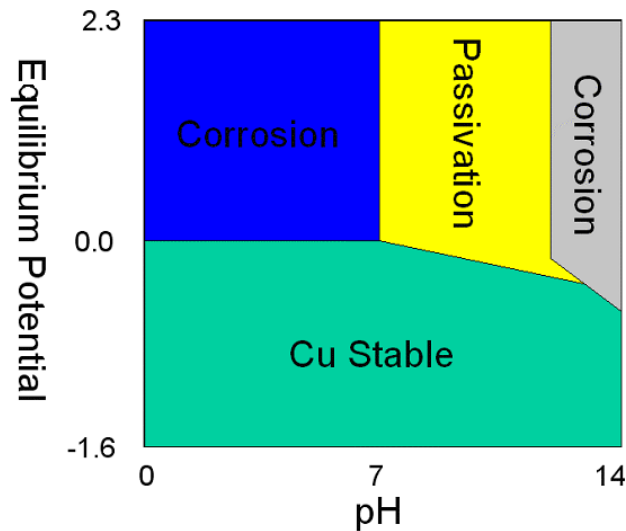


Figure 3. Simplified Pourbaix diagram for copper

As the CAF filament grows (copper ions migrate) along the glass fibre/epoxy interface towards the cathode, an environment of neutral pH is quickly reached. Thus copper precipitates as an insoluble copper salt (left hand edge white region in Pourbaix diagram), and it is this build up of coppers salts that constitute a conductive anodic filament.

The electrochemical reactions described in Section 0 then continue with current flowing along the CAF, and H^+ ions being produced at the CAF. In this way the localised pH gradient moves forward with the CAF growth front.

Completion of conductive pathway

The steps above can all initiate without any serious effect to circuit functionality. Catastrophic electrical failure only occurs when the filaments of copper salts bridge the anode and cathode in question. Under humid conditions the salts are conductive and will allow a massive increase in current flow between the previously well-isolated copper areas, and consequently circuit failure occurs.

Dendritic growth

Dendritic growth is an electrochemical process associated with electro migration on the *surface* of a PCB, and the dendrite grows from the cathode to anode as copper builds up [3]. An image of such a dendrite is shown in Figure 4, and it is important to note this is *distinct and different from CAF* for the reasons described below.

- A dendrite can be seen on the surface of a PCB; a CAF is subsurface
- A CAF is associated with glass filaments; a dendrite is not
- A CAF will grow from an anode to a cathode; a dendrite will grow from a cathode to an anode
- A CAF is created from copper salts; a dendrite is metallic e.g. copper, nickel etc.

It is not possible to see a CAF (even with backlighting) with the naked eye, as is the case for a surface dendrite (although carbonisation as a result of a complete failure if high currents have flowed, may be visible).

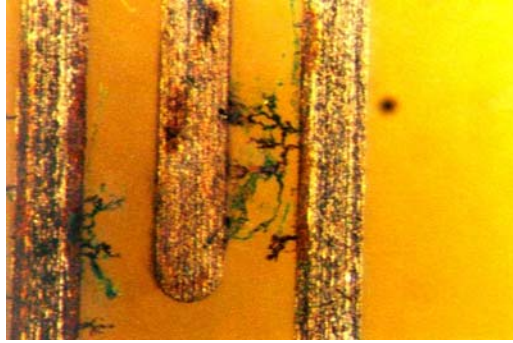


Figure 4. Surface PCA dendrites as a result of flux contamination.

3 EXPERIMENTAL

The work was performed in two phases.

3.1 Phase 1

For Phase 1 all the work was carried out using a standard Tg non-CAF resistance FR4 laminate from laminate supplier L. The processing of this laminate into multi-layer test boards was all performed at board house A.

3.1.1 Test vehicle design

The test vehicle used in Phase 1 was the result of extensive consultation between the project partners. The board has ten-layers and over 6,000 vias. A plot of the Gerber data is given in Appendix A and a manufactured board is illustrated in Figure 5.

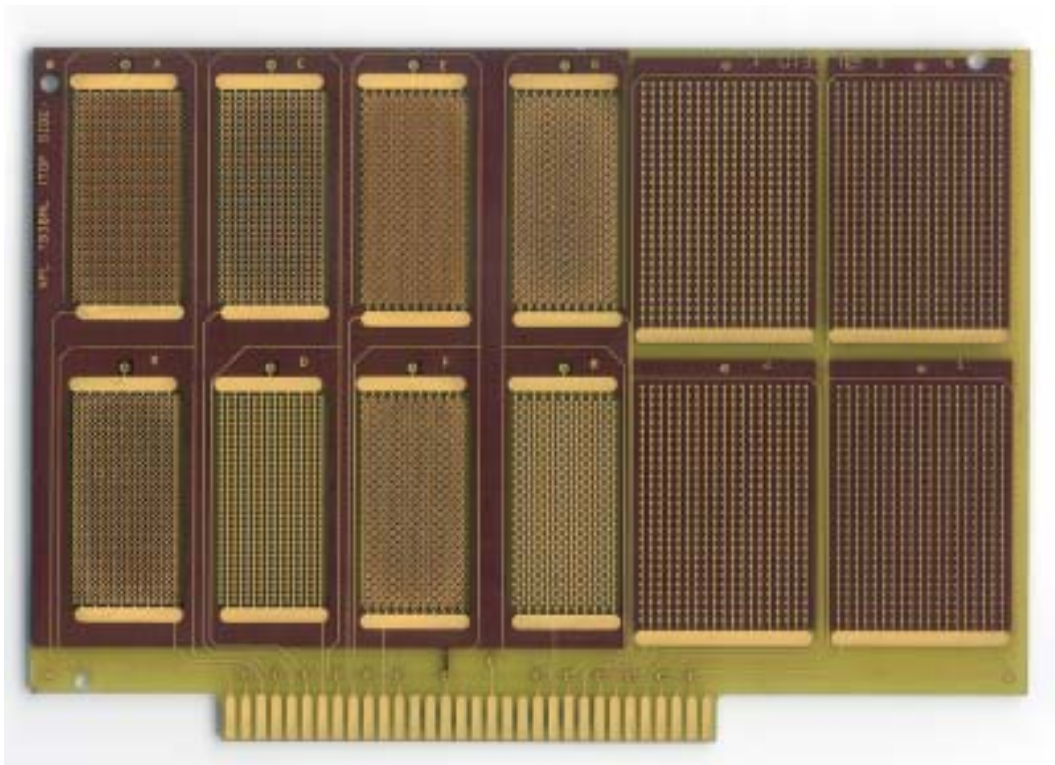


Figure 5. TB38A as manufactured by board house, NiAu finish.

The boards were all made with an electroless nickel immersion gold (ENIG) finish, and no solder mask was applied. The 32-tab connector layout allows connection to a test rack system for application of bias voltage and monitoring of leakage currents. Although the boards had ten layers the design was such that there were only inner-layer pads associated with the through-holes on alternate layers. This was done to avoid the ‘stack of coins’ effect where the additional thickness due to so many identically placed pads can be problematic in the press cycle. The laminate suppliers and board houses ensured that the lay-up of the warp and weft directions on the presses were the same. Microsectioning of the boards validated this.

3.1.1.1 *In-line test combs*

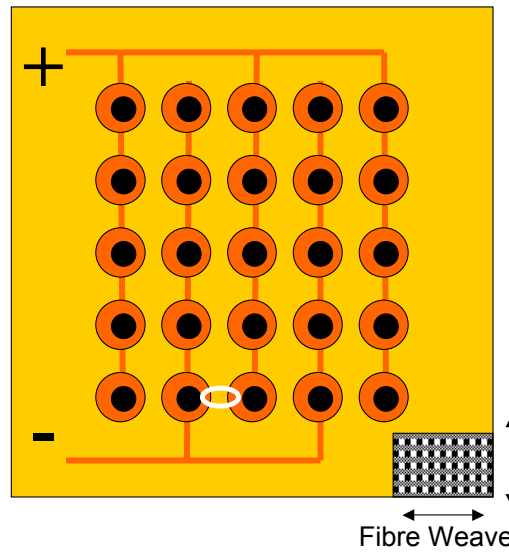


Figure 6. Schematic of in-line test comb, with possible failure site.

The in-line test combs comprised alternate rows of either powered tracks or tracks connected to ground as shown in Figure 6. The via wall to via wall is the most common failure site where CAF can occur. The vias are in line with one another orientated with the glass fibre weave. The closest point between each via pair is the most likely point for CAF growth (example highlighted in Figure 6). The black spots represent the drilled hole, and the copper pads associated with the vias are in orange. Combs A-D in the TB38A design have Gerber specified via wall to via wall distances of 300, 400, 550 and 800 μm . The gap is shown in Figure 7, which is a schematic cross-section of a via pair (note the gap is taken from the edge of the copper plating). It should be noted that the drill size quoted in the Gerber files (shown as A) relates to the hole size after plating. The hole drilled in the laminate prior to plating is in reality about 100 μm wider in diameter to account for the copper thickness.

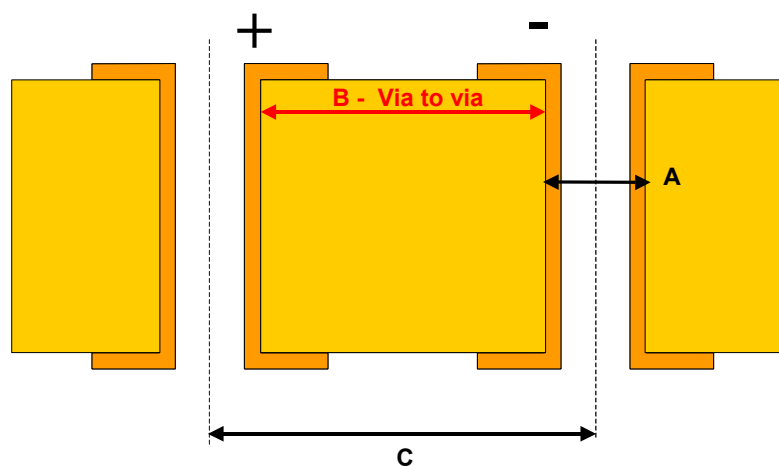


Figure 7. Schematic section of via pair with bias applied.

3.1.1.2 Staggered Combs

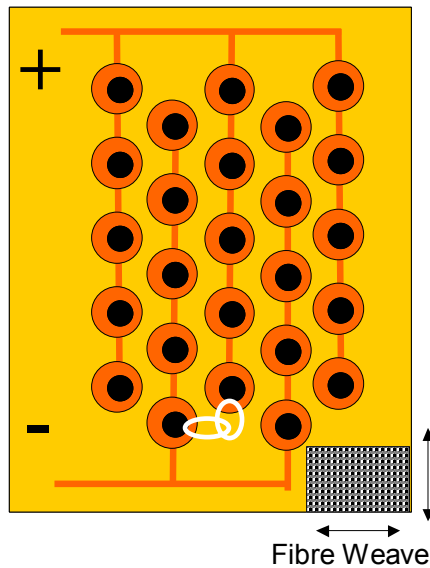


Figure 8. Schematic of staggered test comb, with possible failure site.

The construction of staggered combs (E-H in the TB38A design) is similar to the in-line combs, however the via pairs are arranged at 45° . This means that the most likely route for potential CAF growth is longer since the orientation of the glass fibres may only permit growth in the horizontal and vertical directions (as represented by the white ellipses in Figure 8). The CAF cannot grow at 45° , and must follow the glass filaments.

Combs E-H in the TB38A design had via to via distances of 300, 400, 550 and 800 μm respectively, to retain commonality with the in-line combs.

3.1.1.3 Anti-pad combs

Anti-pads are also potential failure sites where a CAF may grow between a ground plane in a multi-layer board, and a nearby via wall (schematics are shown in Figure 9 & Figure 10). There is a large surrounding copper ground plane at a potential to the through-hole vias.

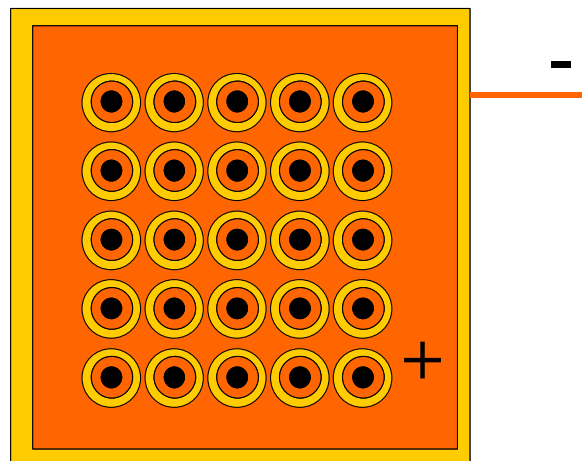


Figure 9. Schematic of anti-pad test comb.

A schematic cross-section of an anti-pad comb is shown in Figure 10. There is no copper ground layer on the surface of the PCB, only in inner layers. Combs I-L on TB38AA are anti-pad style combs. The distance between the inner layer via pads and the ground place (labelled D), often referred to as the ‘anti-pad annulus’ was 100, 125, 175 and 200µm for the combs respectively. The distance between the via wall and the ground plane (E) was the same for all the anti-pad combs.

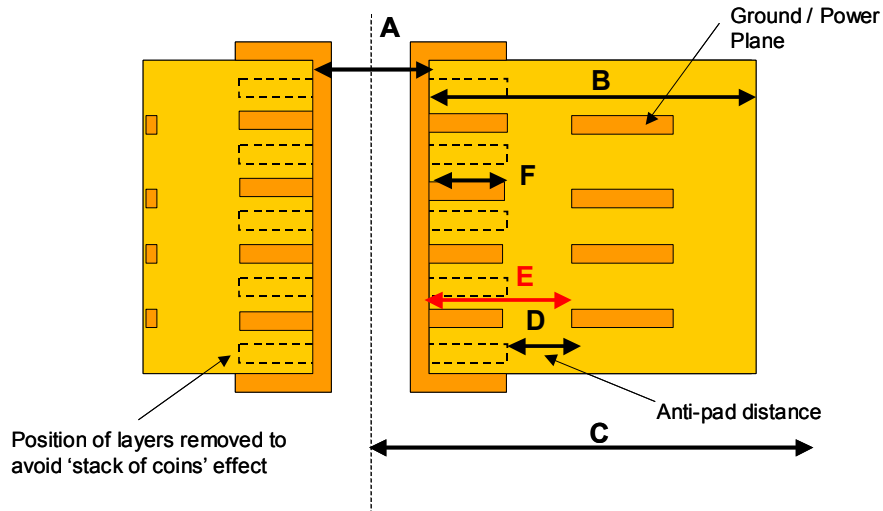


Figure 10. Schematic section of an anti-pad via configuration.

3.1.2 Pre-conditioning of the samples

There were 16 coupons tested in Phase 1. The voltages used and the samples exposed to thermal shock and lead-free reflow profiling are described in Table 1.

Table 1. Thermal exposure conditions for Phase 1 coupons.

No.	Voltage of CAF test	Thermal Shock	Exposure to LF Reflow
1	5	250 cycles	None
2	5	250 cycles	3 passes
3	50	250 cycles	None
4	50	250 cycles	3 passes
5	150	250 cycles	None
6	150	250 cycles	3 passes
7	500	250 cycles	None
8	500	250 cycles	3 passes
9	5	None	None
10	5	None	3 passes
11	50	None	None
12	50	None	3 passes
13	150	None	None
14	150	None	3 passes
15	500	None	None
16	500	None	3 passes

3.1.2.1 Thermal shock

Thermal shock equipment comprised a dual silicone oil bath system. The baths were held at -15°C and $+120^{\circ}\text{C}$ and the coupons were transferred between the baths by a robotic arm. The thermal shock cycle time was 14 minutes with a 5-minute dwell in each bath. The selected samples were exposed to 250 thermal shock cycles.

3.1.2.2 Lead-free reflow exposure

Selected test coupons were exposed to three passes through a five zone forced convection reflow oven, configured for lead-free processing.

Using a thermocouple placed on the PCB the board temperature through the profile was monitored, and a typical reflow profile is shown in Figure 11. The boards were allowed to return to room temperature after each pass before being passed through the oven again [4].

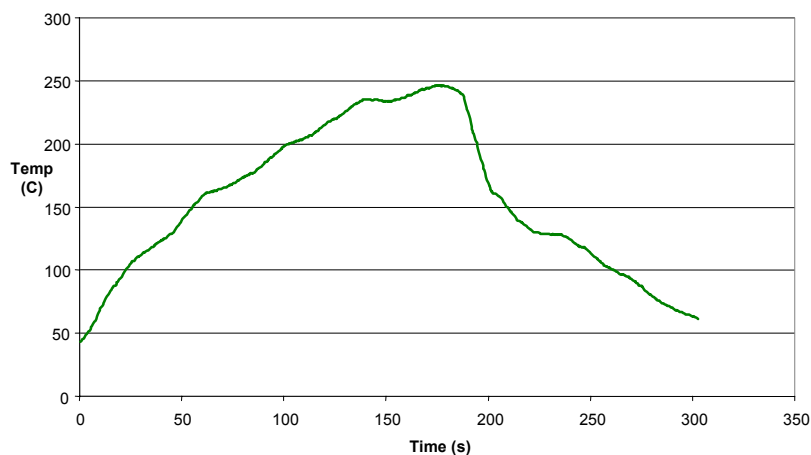


Figure 11. Thermal profile for TB38A board, measured at corner of board.

3.1.3 Artificial ageing and resistance monitoring

The samples were placed in an environmental chamber and run up to a steady state condition of 85°C and 85%RH and exposed for 1000 hours. During the initial ramp, the temperature was increased ahead of the relative humidity, to prevent any condensation on the samples.



Figure 12. CAF test coupons under test in environmental chamber.

Throughout the 1000-hour exposure the insulation resistance (IR) of each comb pattern (192 combs in total) was measured and logged every 20 minutes. The resistance measurement system was a 256 channel Auto-SIR™ using a current limiting resistor of $10^6\Omega$.

3.2 Locating, sectioning & analysing CAF

After failures had been identified using the electrical monitoring technique, comb C on test coupon No.11, (In-line via, 50V, 0 thermal cycles, 0 reflows, 500 μ m actual gap) was selected for sectioning to locate and identify the CAF. This allowed confirmation that the electrical short detected was associated with a CAF failure, and underlined the general approach of using electrical measurements to detect a CAF. The procedure for discovering a CAF is described below.

Electrical isolation

Once the comb was out of the chamber a Keithley 237 high voltage measurement source was used to apply 10V across the selected comb pattern with the current limited to 10 μ A. The pair of vias that had shorted were located by progressively isolating areas of the comb by cutting the surface copper tracks with a scalpel blade, and re-testing for a low resistance ($<10^6\Omega$).

The boards were tested straight from the chamber as conductivity of the CAF can decrease in some cases as the laminate dries out. After 10 minutes the laminate was returned to the chamber at 85°C and 85%RH for 30 minutes before location of the failed via pair commenced.

Sectioning and polishing

The area between the failed vias was cut using a slow speed, wet diamond saw, very close to the anode via wall, as indicated in Figure 13.

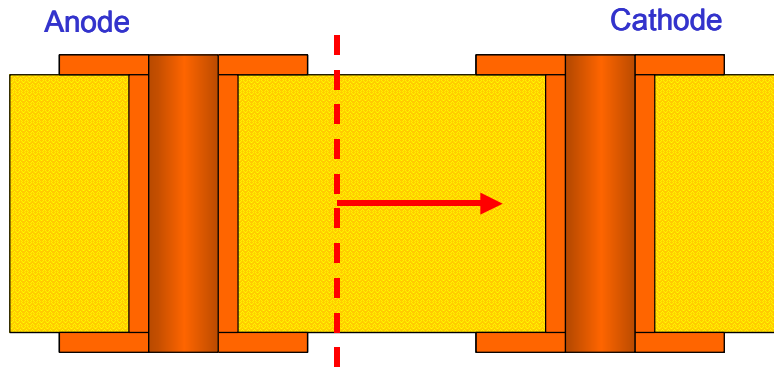


Figure 13. Schematic section to illustrate polishing to locate CAF.

Sequential polishing with 5 to 1 μm particle polish was then used to move through the sample towards the cathode. Between each stage of polishing the sample was examined through an optical microscope until the CAF was located.

Analysis of CAF

After a high-resolution optical image of the CAF cross-section was acquired the polished CAF sample was carbon coated and mounted for EDAX analysis in an SEM. The filament area was analysed for elemental composition and an elemental digi-map produced for correlation with the optical image.

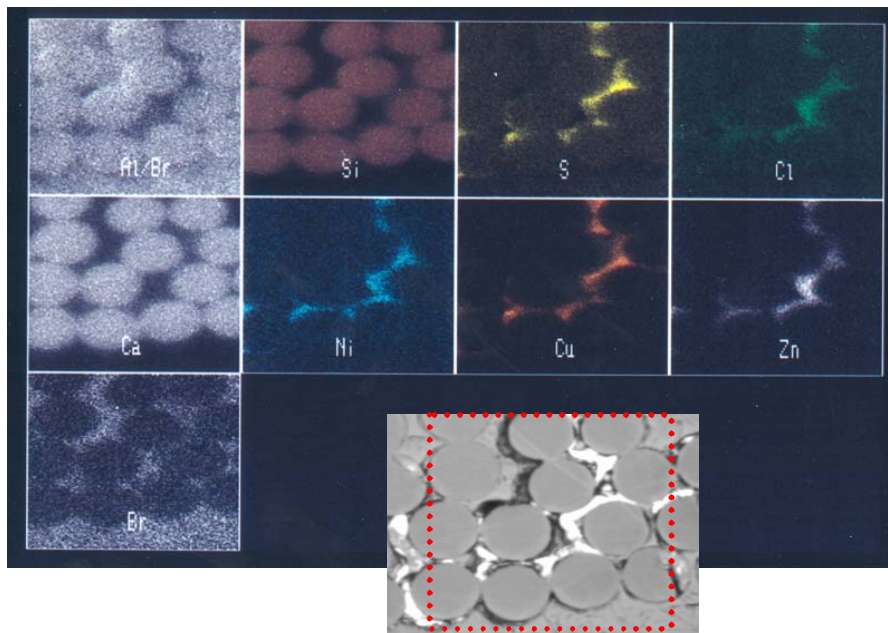


Figure 14. Optical and EDAX images of microsection showing presence of many elements associated with the CAF

This shows that electrical measurements correlated to the physical presence of CAFs in the samples.

3.3 Phase 2

From Phase 1 a number of test conditions were decided, e.g. voltage, geometries etc. In Phase 2 the aim was to establish how various board parameters influence CAF susceptibility. These results were then used to verify or modify the test procedure, as appropriate. The board parameters tested were: laminate type, PCB board house; PCB Tg; CAF resistance resin formulations; PCB solderability finish; mechanical drill feed speed, and PCB reflow conditions. In Table 2 the 42 PCBs tested are listed with various assigned experimental parameters. The parameters are described in the following Sections. The boards 40, 41 and 42, and designated M, were obtained by a project partner and supplied as a commercial product.

Table 2. Experimental matrix for Phase 2, including material and processing variables.

Sample No.	Board House	Laminate Supplier	TG	CAF RES?	WEAVE	FINISH	DRILL FEED	Reflow					
1	A	K	High	Yes	2116	NiAu	1	3 x LF					
2			None										
3			High	No				Yes	None				
4										3 x SnPb			
5										3 x LF			
6			Low	Yes				Yes	None				
7		3 x SnPb											
8		3 x LF											
9		L	High	Yes				Yes	None				
10										3 x SnPb			
11			Low	No				No	None				
12										3 x LF			
13										3 x SnPb			
14	B	K	High	Yes	2116	1	3 x LF						
15								NiAu					
16								Ag					
17								HASL					
18								OSP					
19			NiAu										
20			Ag										
21			HASL										
22			OSP										
23			NiAu										
24		L	High	Yes				No					
25									L	Low	No		
26		K	High	No				Yes	2113	NiAu			
27											K	Low	Yes
28											L	High	Yes
29	C	K	High	Yes	2116	NiAu	1						
30								High	No				
31								Low	Yes				
32		L	High	Yes				Yes	1				
33										High	Yes	Yes	2
34													
35										Low	No	No	4
36			1										
37				2									
38			3										
39				4									
40	M							None					
41								3 x SnPb					
42								3 x LF					

3.3.1 Laminate supplier

There are various aspects of the laminate considered, but in this study the effect of having independent suppliers was investigated. The laminate supplier here is defined as the company providing the base laminate materials (pre-preg layers, cores etc) to the board house; there were two in this project. A schematic of the basic process for the manufacture of glass-reinforced epoxy is shown in Figure 15. The warp bundles are those in line with the rollers which are generally held under more tension than the weft bundles which are perpendicular to the process flow.

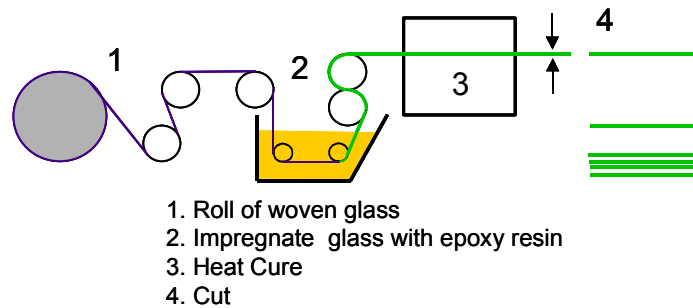


Figure 15. Simplified schematic of composite glass-reinforced epoxy.

3.3.2 Board house

The board house manufactures the PCBs, using the Gerber design data to etch, drill and plate copper foils. The materials are placed in a press cycle to bond all the layers together forming the multi-layer board. There a plethora of chemical preparation, etching, drilling, alignment, masking and development stages which take place during the construction of a multi-layer PCB, and a simplified schematic is given in Figure 16.

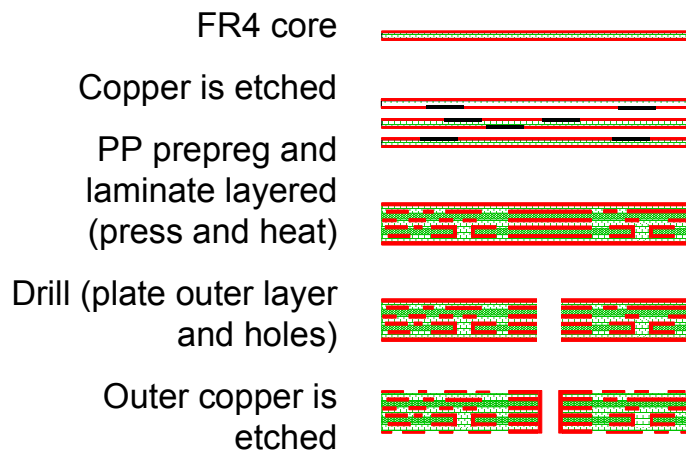


Figure 16. Simplified schematic of multi-layer PCB construction.

3.3.3 Glass transition temperature (T_g)

The glass transition temperature (T_g) marks the onset of segmental mobility for a polymer. Below this temperature the polymer segments do not have sufficient energy to move past one another and the material properties are essentially glass-like. In practice for FR4 laminates, rigidity and co-planarity can be affected once the T_g is exceeded by a large margin.

3.3.4 CAF resistance

Suppliers can offer laminates that use resin cure systems to reduce the likelihood of CAF formation in product and are marketed as CAF resistant. A known contributor to the problem is the curing agent dicyandiamide (DICY), which is eliminated from such materials.

3.3.5 Weave

The weave refers to the make up of the glass fibres, or filaments, in the woven construction used in the composite. Single glass filaments are bundled into strands. A number of strands are then taken and woven. The numbers of strands (also known as threads) in the warp and weft directions of the weave are not necessarily equal, and the total number is varied depending on end application. There were three glass weave types used in this study: 2116, 2113 and a commercial laminate of unknown weave style. The properties of the glass weaves (warp/weft) are given in Table 3.

Table 3. Properties of glass-reinforced weaves.

Style	Tensile Strength (Kgs/cm)	Woven Cloth Thickness (mm)	Weight (g/m ²)	Threads per cm warp/weft	Filament Diameter (µm) warp/weft	Filaments per Strand warp/weft
2116	15 x 11	0.1	105	24 x 23	7\7	225/225
2113	15 x 8	0.07	83	24 x 25	5/5	408/204

3.3.6 Board finish

A protective finish is required to keep the copper surface of the PCB solderable after storage. This is another process typically carried out by the board house. In this study the following finishes were used:

- **ENIG** – Around 2 to 3µm of Ni as a protective barrier with around 0.1µm of Au to protect the nickel
- **Ag** – 100nm of a silver organic compound covers the copper
- **HASL** – (Hot air solder levelling). Tin-lead solder is used to cover the copper areas, and is levelled with a hot air knife before it solidifies to help keep the coverage as level as possible. Thickness is typically 2-4µm.
- **OSP** – (Organic solderable preservative). This high molecular weight organic layer provides resistance to degradation, covers the hole board surface, and is designed to be removed by subsequent soldering steps.

3.3.7 Reflow

This is a circuit assembly production step for soldering components to the PCB. In Phase 2 three different reflow conditions were applied:

- No Reflow – As a control condition
- SnPb Reflow – A heating profile typical of that used to reflow solder paste with SnPb alloy (eutectic 183°C)
- Lead-Free Reflow - A heating profile typical of that used to reflow solder paste with SnAgCu lead-free alloy (eutectic ~217°C).

3.3.8 Test vehicle design - TB38B

The test vehicle used in Phase 2, TB38B, included some alterations and improvements to TB38A. The track outs from the combs were altered to allow isolation of the failure (by track cutting) not only by via pair, but also by board layer. A plot of the Gerber data is given in Appendix B and a manufactured board is shown in Figure 17, with the comb areas labelled.

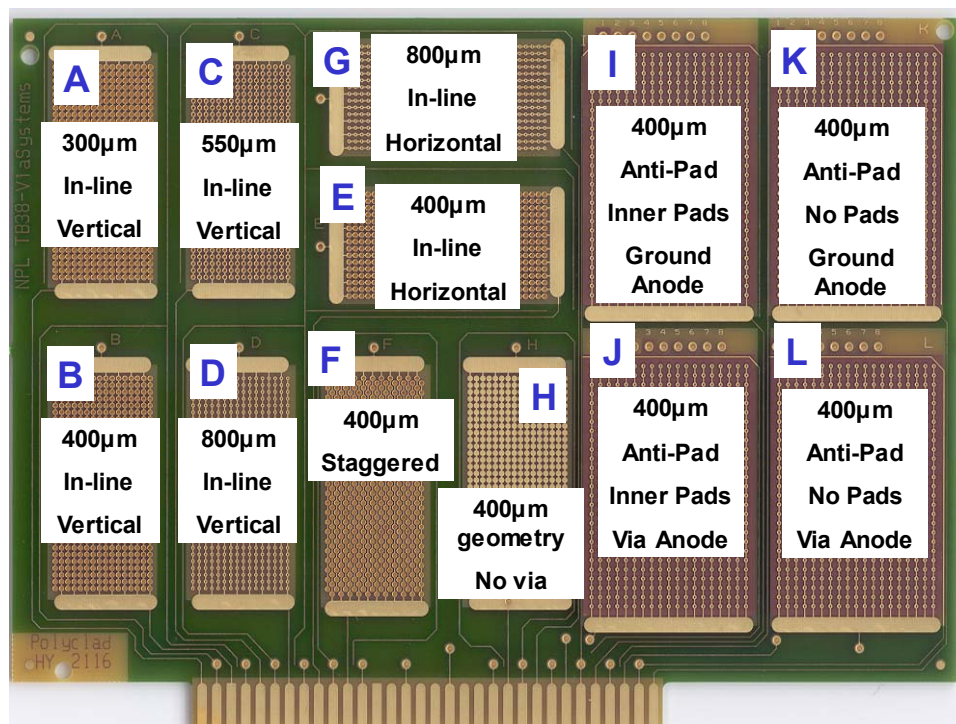


Figure 17. TB38B, as manufactured by board house, NiAu finish.

3.3.8.1 In-line test combs

The in-line test combs A-D remain unchanged from the TB38A design, since they proved to give earliest failures and definitive trends with gap size. Two new in-line combs (E, 400µm gap, and G, 800µm gap) were added to combs B and D, but with an orientation at 90° to the other combs. This was done to investigate any differences in the CAF susceptibility might be sensitive to orientation between the warp and weft glass bundles.

3.3.8.2 Staggered combs

Only one staggered comb (F) was used on the TB38B design with a 400 μ m gap.

3.3.8.3 Anti-pad combs

There were four anti-pad comb patterns in the TB38B design. Due to the progress made in Phase 1, the main interests for Phase 2 were in the effects of the direction of CAF growth, and in understanding more about the effects of the presence of inner layer pads. Figure 18 then, presents the configuration of combs I, J, K and L. The dimensions, apart from the changes in the presence of pads, are the same for all four anti-pad style combs. I and J are a pair, but with the polarity reversed, as are K and L. I and J have anti-pads, whereas K and L do not.

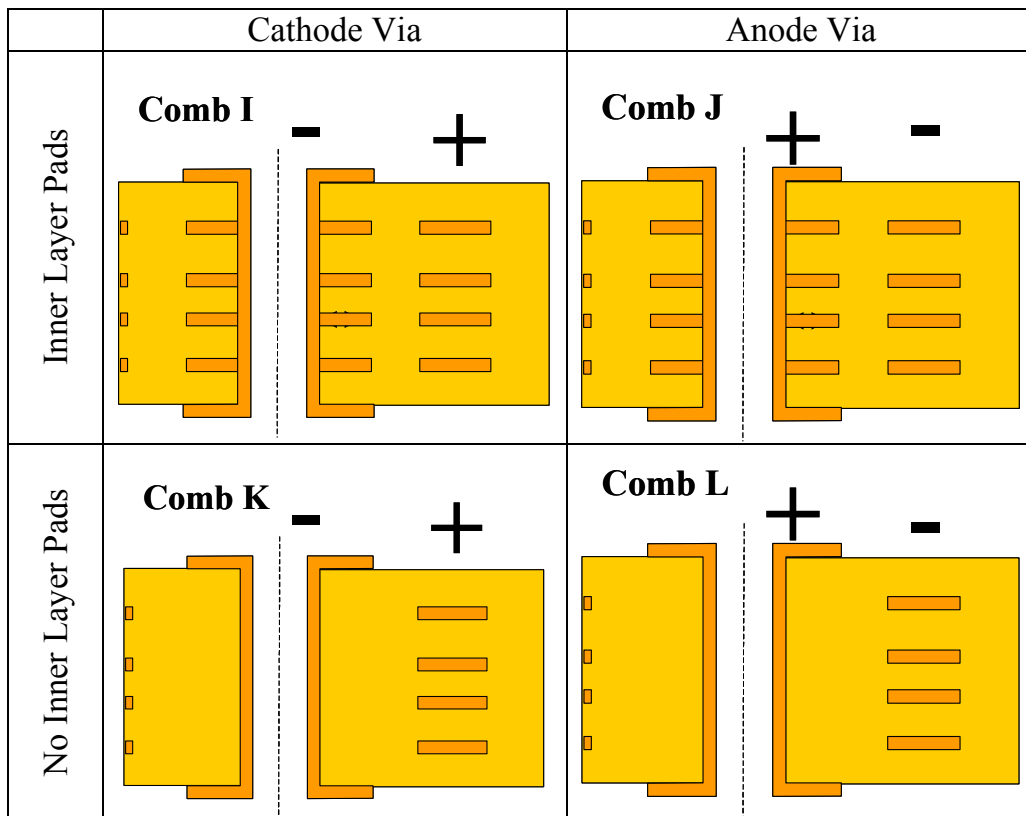


Figure 18. Schematics show the configuration for anti-pad combs I, J, K and L in TB38B design.

3.3.9 Pre-conditioning of the samples

Forty two test coupons were exposed to reflow profiling as described in the 'Reflow' column of Table 2.

3.3.10 Artificial ageing and IR monitoring

The procedure and conditions for artificial ageing and IR monitoring were the same as used in Phase 1, see Section 3.1.3.

4 RESULTS AND DISCUSSION

A typical insulation resistance (IR) vs. time curve for a failed comb, measured during the 1000 hours accelerated ageing, is shown in Figure 19.

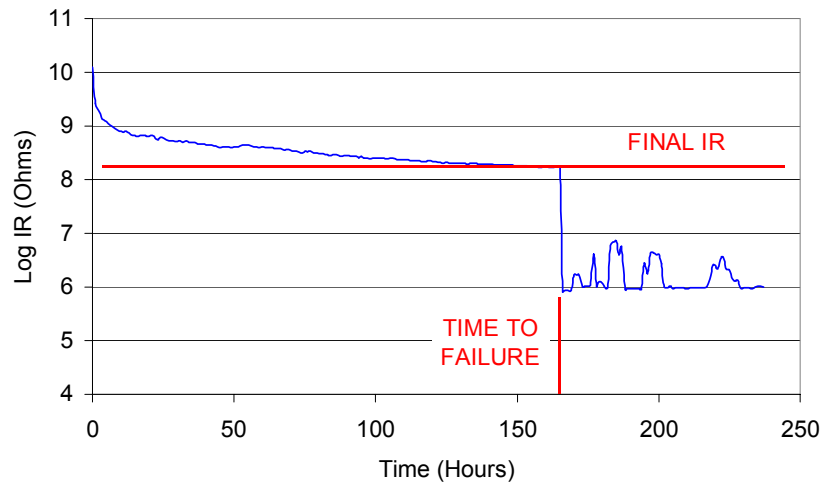


Figure 19. Example of the electrical effect of a typical CAF failure.

The decrease in IR as moisture permeates the laminate material can be seen in the first 10-20 hours of the test. At about 170 hours (in this example) there is a sudden catastrophic loss in insulation between the through-hole vias in the comb. The IR does not drop below $10^6 \Omega$ due to the use of a current limiting resistor in the measurement instrument.

Two parameters can be noted from the IR-time curve for each comb tested in this work, the final IR (log Ohm) and the time to failure (hours), as indicated.

4.1 Phase 1

4.1.1 Trends in time to failure

In this Section the ‘time to failure’ results for Phase 1 are plotted on three-dimensional axis. By plotting in this way the effect of varying the via wall to via wall distance and the applied voltage can be easily seen. Blue areas represent a fast time to failure, through to red indicating a long time to failure. If the comb pattern did not fail at 1000 cycles then the plot area is black (reference Figure 21). For very quick failures at high voltage and small gaps the boards were inspected for ‘flash over’ where the high voltage gradient and humidity induced dielectric breakdown of the laminate (example Figure 20). This of course is not CAF but explains the few ‘zero’ failure times observed.

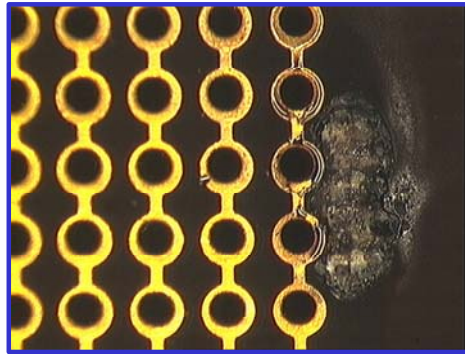


Figure 20. Example of 'flash over', normally encountered with small gaps and high voltage.

4.1.1.1 In-line vias

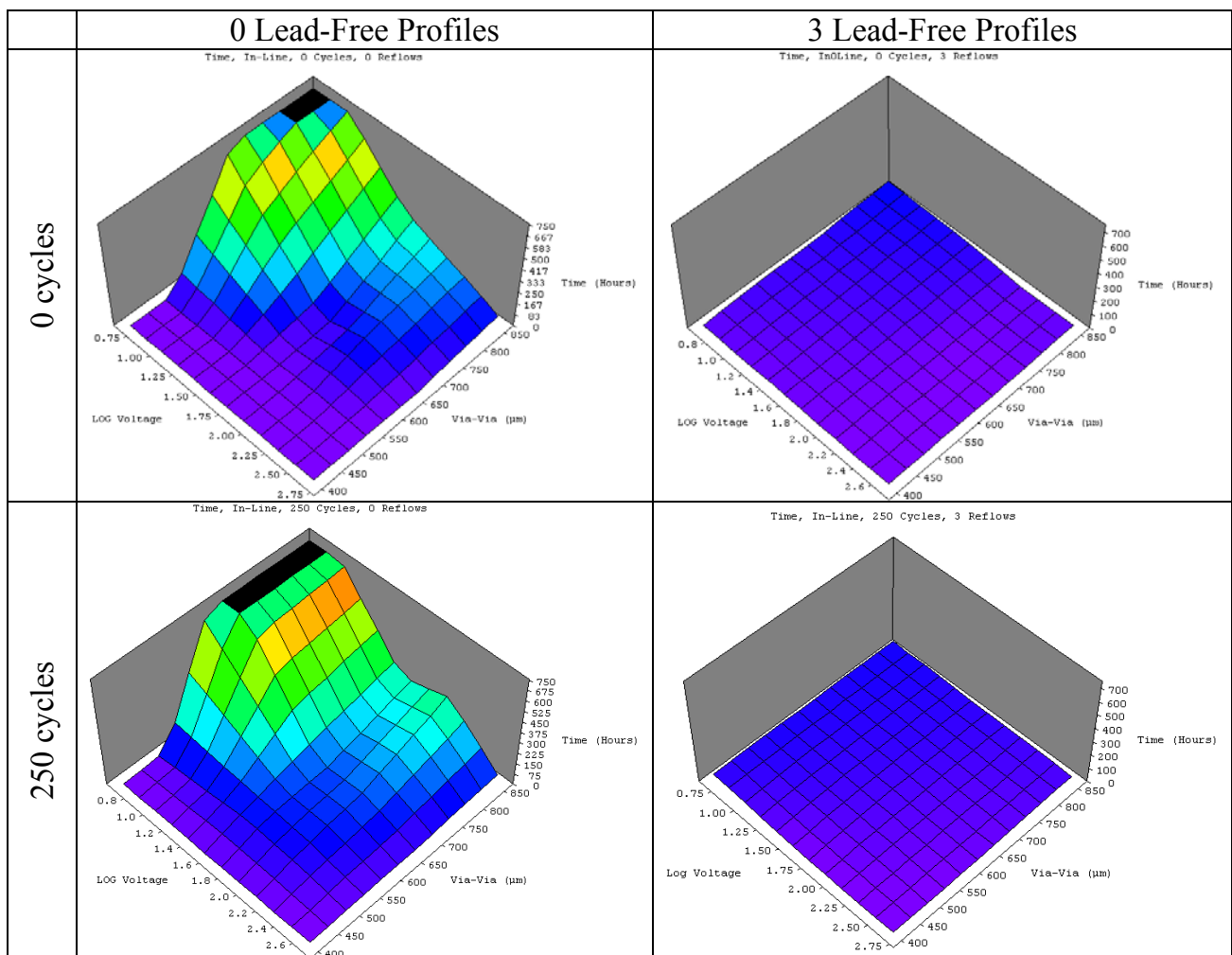


Figure 21. Effect of geometry, voltage and thermal exposures for standard FR4, in-line vias.

In Figure 21 four 3D-plots are shown for the in-line comb patterns. There is a trend in all samples for higher voltages and smaller via to via gaps to cause earlier failures, (causing the plotted surface to slope from back to front).

The plots show the effects of preconditioning the samples with thermal shock and lead-free profiling. By comparing the upper and lower rows the negligible effect of thermal shock cycling on time to failure can be seen. In contrast, a comparison between the two columns highlights the significant decrease in time to failure caused by exposure to lead-free profiling. *This will be an important issue as reflow temperatures are pushed upwards for lead-free reflow processing.*

4.1.1.2 Staggered vias

In Figure 22 four 3D-plots are shown for the staggered comb patterns. There is again a trend in all samples for higher voltages and smaller via to via gaps to cause earlier failures, (causing the plotted surface to slope from back to front). It is important to note the in-line and staggered combs are designed so that the via to via gaps are the same and the two Figures can be directly compared. A comparison between the two columns highlights a slight decrease in time to failure caused by exposure to lead-free profiling. *The effect of the lead-free profiling is a lot less significant than in the case of the in-line vias.*

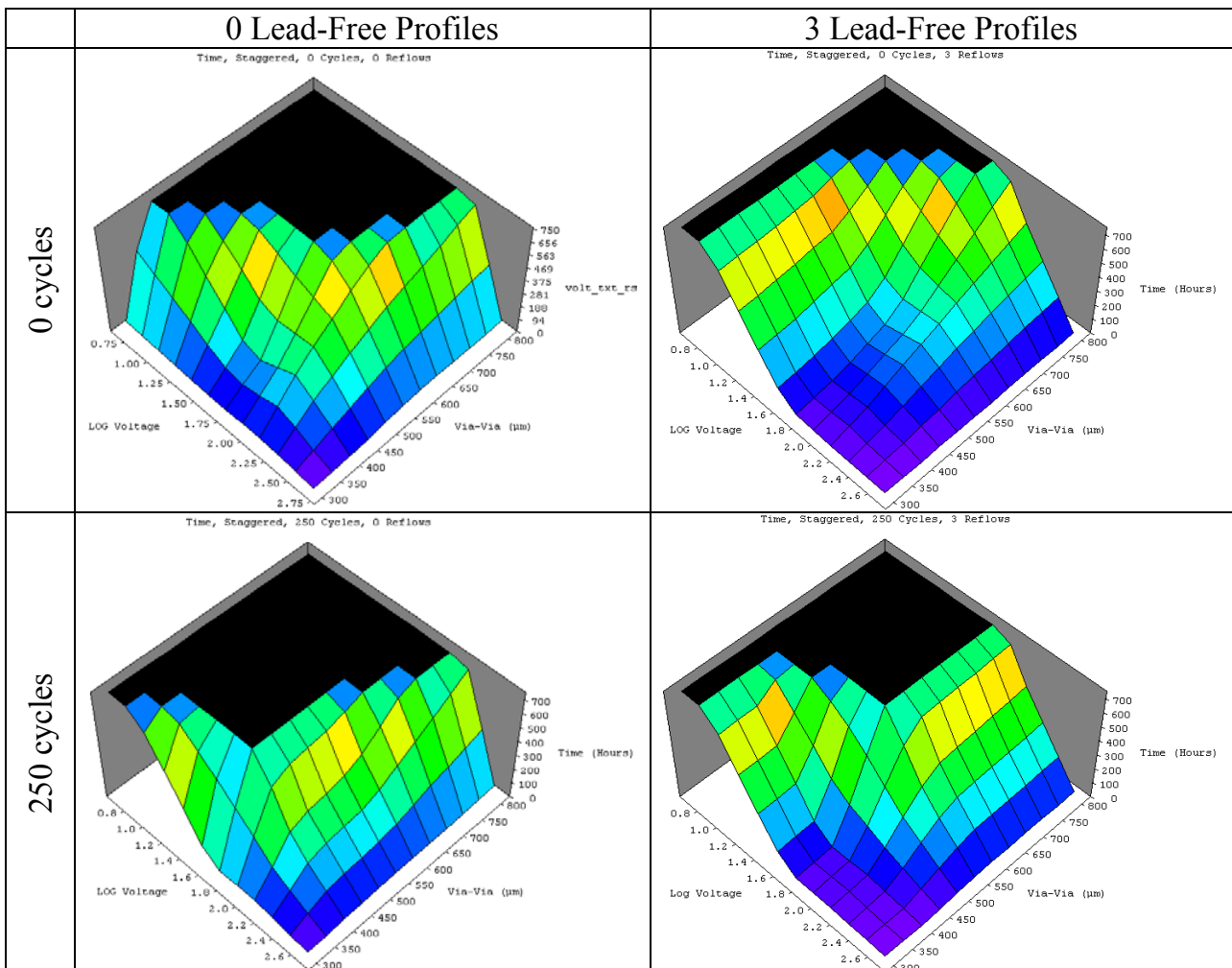


Figure 22. Effect of geometry, voltage and thermal exposures for standard FR4, staggered vias.

4.1.1.3 Anti-pad vias

In Figure 23 four 3D-plots are shown for the anti-pad comb patterns. There is again a trend in all samples for higher voltages to cause earlier failures, (causing the plotted surface to slope from back-left to front-right). However, there is no dependence on anti-pad dimensions, whereas for the in-line and staggered patterns there was a strong dimensional effect.

The plots show minor decreases in CAF resistance due to thermal shock and lead-free profiling.

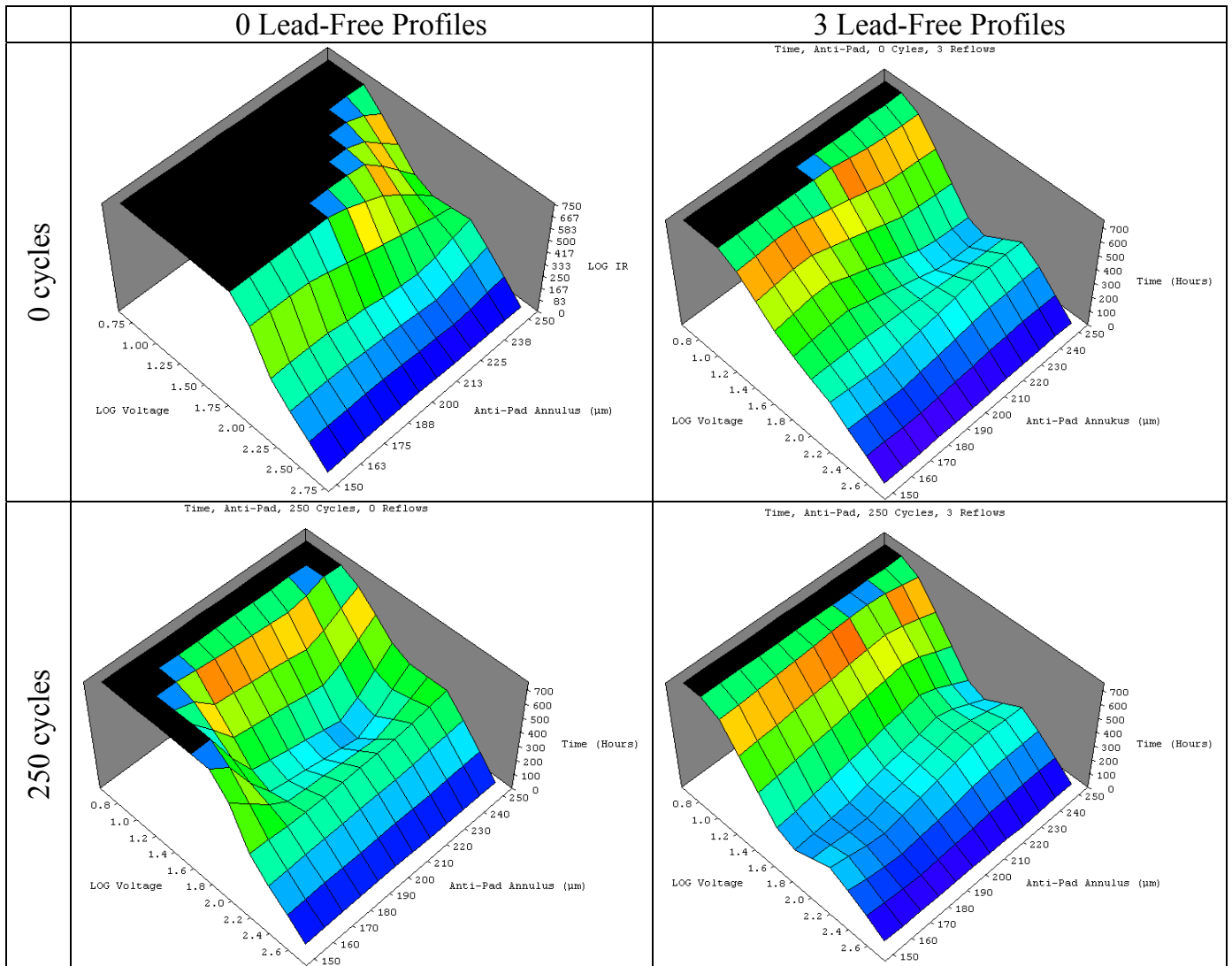


Figure 23. Effect of geometry, voltage and thermal exposures for standard FR4, anti-pad vias.

4.1.2 Insulation resistance

The final insulation resistance (IR) values were recorded because it was hoped they might provide some performance metric. Clearly it would be advantageous if the IR remains high for as long as possible. The insulation resistance results for Phase 1 are similarly plotted on three-dimensional axis as illustrated in Figure 24. By plotting in this way the effect of varying the via to via distance and the applied voltage can be easily seen, and compared with the times to failure in Figure 23.

4.1.2.1 In-line vias

In Figure 24 four plots are shown for the in-line comb patterns. The consistency in results is less than for the time to failure data. IR appears independent of voltage and dimensions, with the exception of very small via wall gaps, as already associated with rapid non-CAF failures (Figure 20). The impact of thermal shock and lead-free reflow on IR appears to be insignificant, in contrast to the negative impact of LF reflow on time to failure (Section 4.1.1.1). *The suggested use of IR as a CAF indicator would not be appropriate for detecting the damage to the laminates due to lead-free profiling, and as such it would be a poor indicator of performance.*

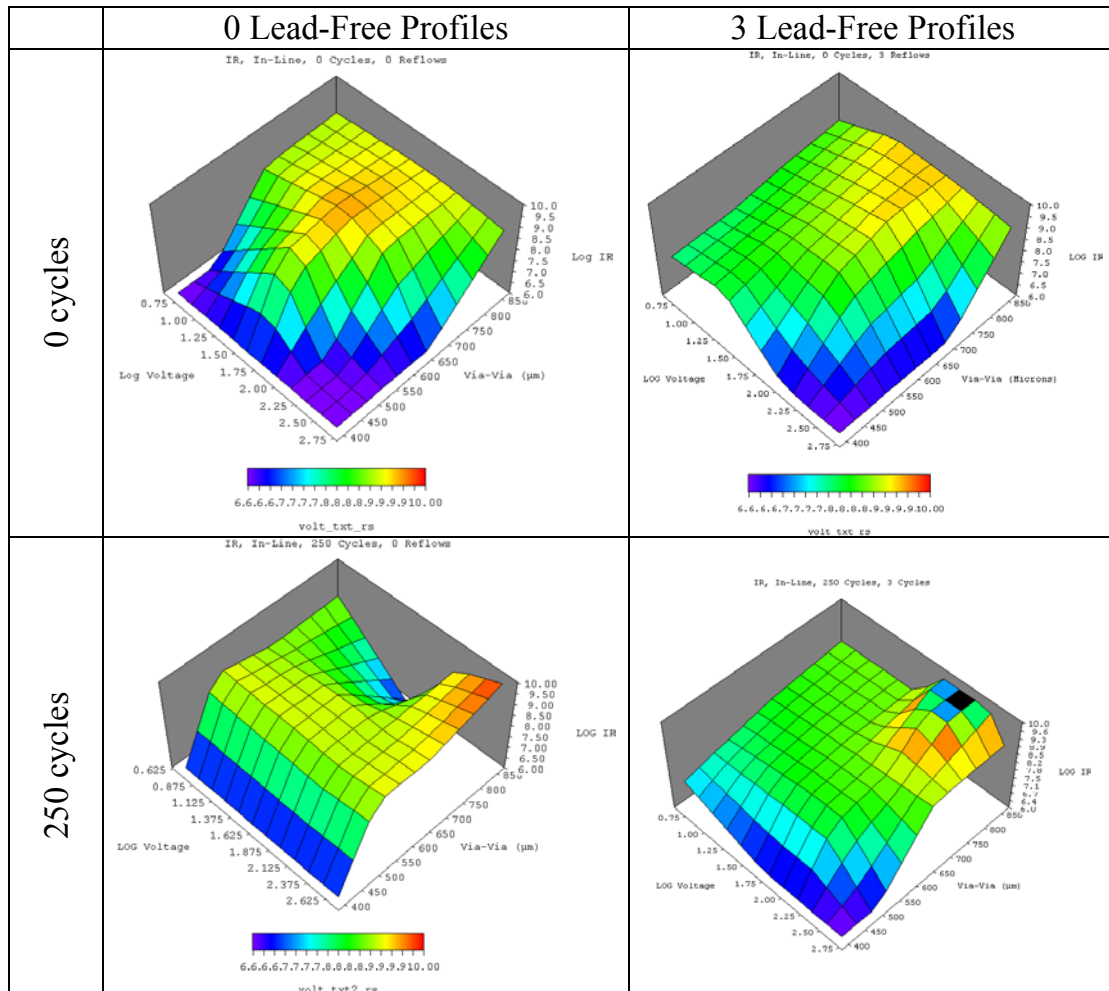


Figure 24. Effect of geometry, voltage and thermal exposure on IR, in-line vias

4.1.2.2 Staggered vias

In Figure 25 four plots are shown for the staggered comb patterns. Interestingly the IR is generally higher for the same voltage and gap conditions than for the in-line vias, correlating with the longer failure times for the staggered configurations (Section 4.1.1.2). Marked drops in IR were only observed with small gaps, and high voltages. *The impact of thermal shock and lead-free reflow on IR appears to be insignificant, in contrast to the negative impact of lead-free reflow on time to failure (Section 4.1.1.2).*

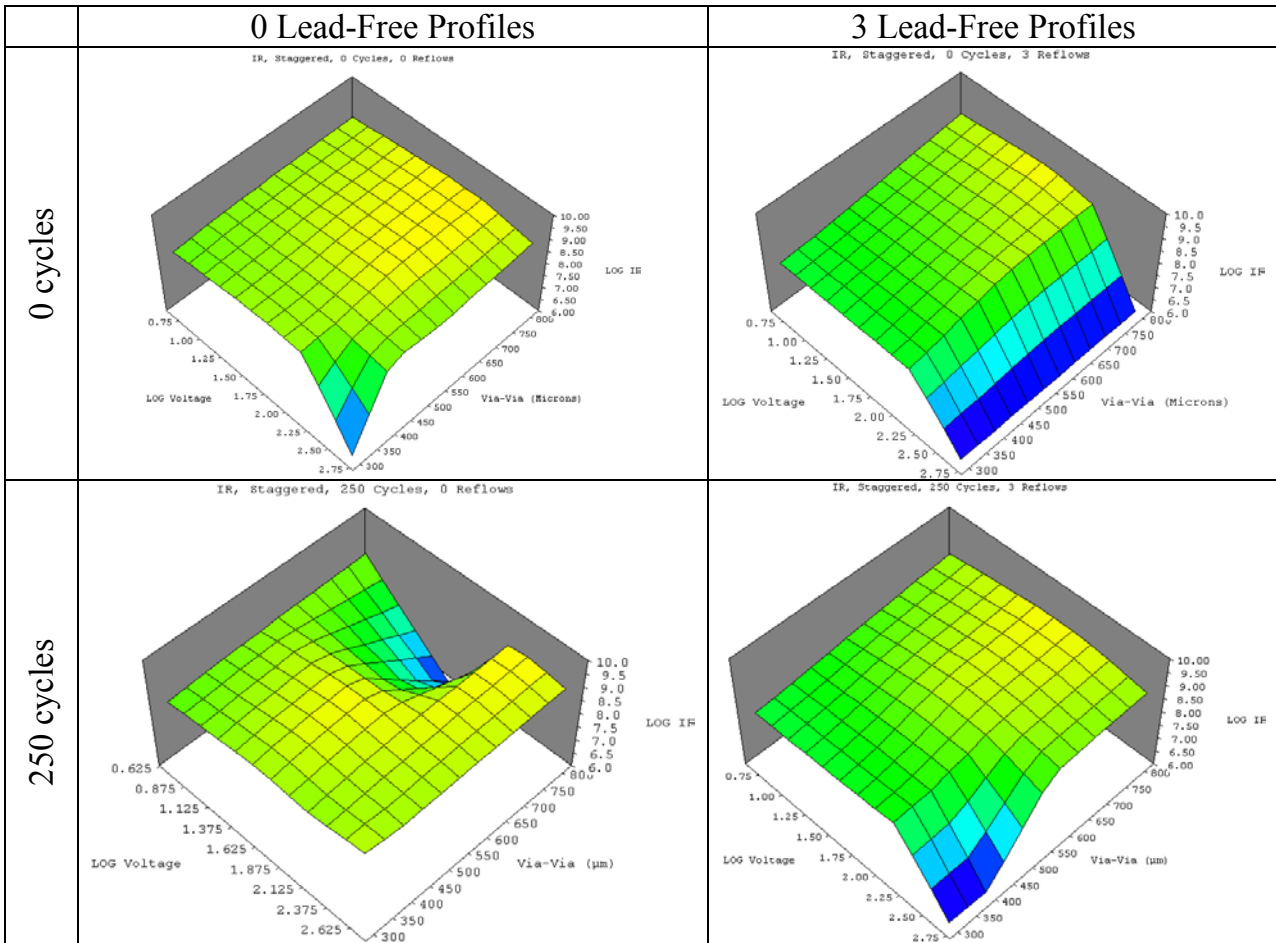


Figure 25. Effect of geometry, voltage and thermal exposure on IR, staggered vias

4.1.2.3 Anti-pad vias

In Figure 26 four 3D-plots are shown for the anti-pad comb patterns. There is no significant effect of voltage, anti-pad annulus size, thermal shock, or lead-free profiling on the IR between the via and the ground plane. *Clearly measuring insulation resistance does not give any indication of, or correlation with time to failure for these comb patterns.*

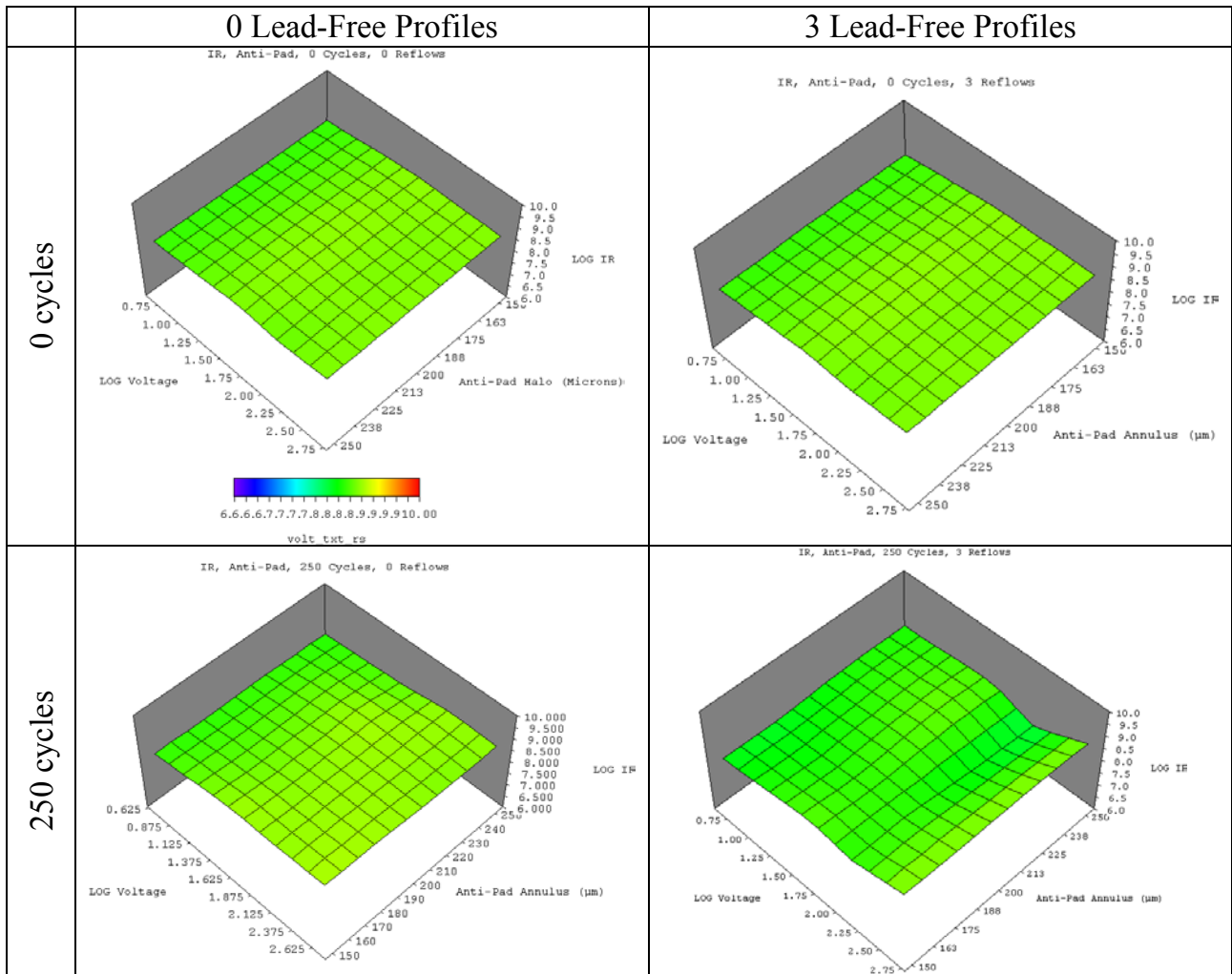


Figure 26. Effect of geometry, voltage and thermal exposure on IR, anti-pad vias

The lack of any effect of the inner layer pad size suggests that the failure route lies between the via wall and the ground plane, rather than the pad and the ground plane, since this distance remains constant in all the combs. Figure 27 illustrates this idea, the full lines indicating where failures were expected, and the dashed lines indicating where they may have taken place.

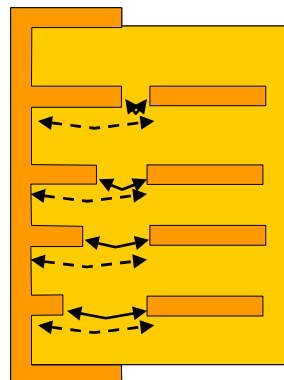


Figure 27. Independence of time to failure to anti-pad gap suggests growth to/from via wall.

4.1.3 Summary of Phase 1, and influences on Phase 2

One of the important decisions from Phase 1 was that IR was not useful as an indicator of CAF susceptibility for laminates, and so it was not pursued into the next phase of work. It was clear that voltage and via to via distance were key variables, and that reflow conditions could have an effect of CAF susceptibility.

The clear trend showing in-line combs, as ‘weakest link’, would mean that these should be retained as the main test comb format. A shortcoming of the TB38A design was noted in that it was unable to discriminate between the properties of the warp and weft fibre directions. The Phase 2 design addressed this concern.

The data for the anti-pad combs showed that they were insensitive to anti-pad distance, thus Phase 2 investigated this further, and also considered bias reversal.

From Phase 1 data an understanding of CAF behaviour was established for standard laminates, and provided a basis for the refinement of the test vehicle in Phase 2, and further investigation of the laminate and processing variables.

4.1.4 Normalisation to voltage gradient

In many instances designers use voltage gradient as a parameter for the limits of performance for board materials. Dielectric breakdown data for bulk insulators are often presented in this format. In this Section the parameters of voltage and gap were combined into voltage gradient. TTF results were then plotted using voltage gradient to compare different comb designs.

TTF data for a series of in-line via designs are given in Figure 28, plotted against voltage gradient. For voltage gradient to be a useful indicator for the prediction of CAF failure there should be a good correlation between TTF and voltage gradient for a wide range of geometries. Figure 28 shows there is no such correlation, with smaller via geometries failing earlier than larger geometries under the same applied voltage gradient.

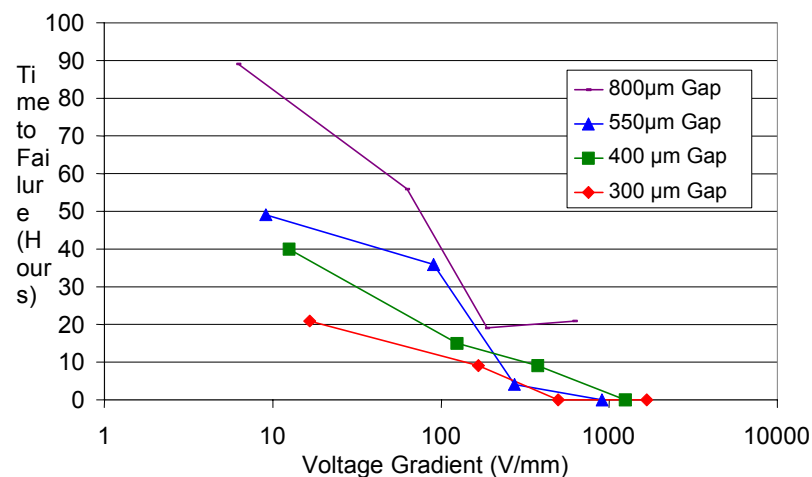


Figure 28. The effect of wall-to-wall gap on TTF, (in-line, no cycling, 3 reflows)

Data for staggered vias show the same effect (see Figure 29) indicating that voltage gradient is not a good predictor of CAF TTF.

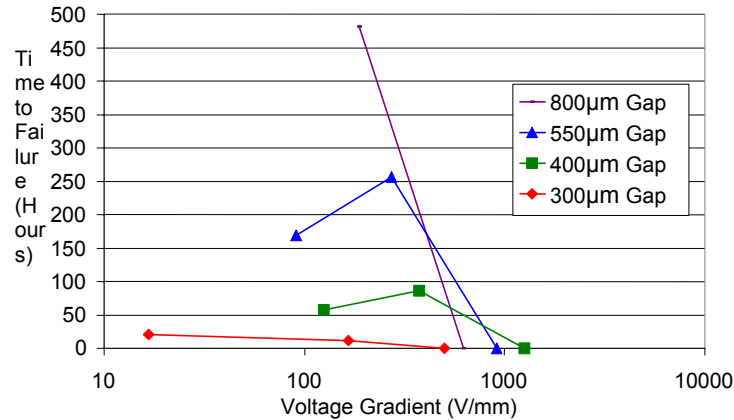


Figure 29. The effect of wall-to-wall gap on TTF, (staggered, no cycling, 3 reflows)

4.1.5 Real-time plots

The monitoring equipment used allowed accurate monitoring of IR of the comb patterns throughout the 1000 hours testing runs. The growth of a CAF requires an electrochemical reaction and thus an associated flow of current (Section 0). Using a resistive cylinder model (Figure 30) the distance that the CAF has grown at any point during the test can be estimated from the change in resistance between the plated through-hole walls. The model assumes a negligible resistance for the CAF filament, meaning the insulation provided is simply proportional to the distance the CAF has left to cover.

$$\%Dt = \frac{R_i - R_t}{R_i - R_f} \cdot 100$$

Where:

- %Dt = Percentage of wall-to-wall distance travelled at time t
- R_i = Initial resistance once steady state conditions are stabilised
- R_t = Insulation resistance at time t
- R_f = Final resistance just prior to sudden IR loss due to bridging of CAF

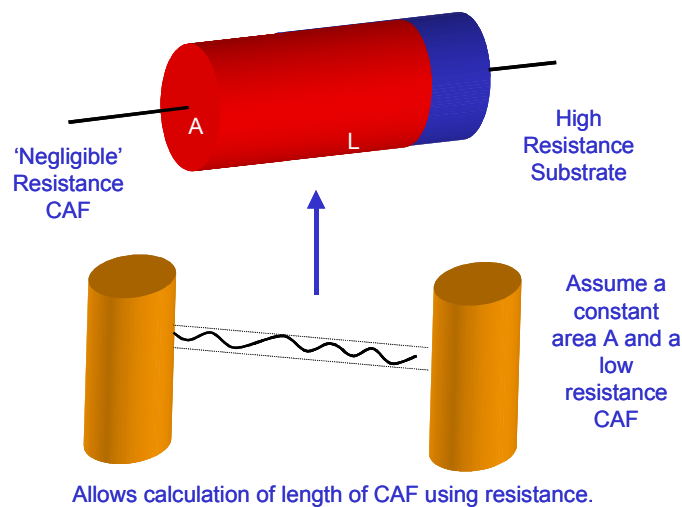


Figure 30. Schematic showing assumption made using a resistive cylinder model

This simplistic model takes no account of any conductive region, and there are many assumptions made that must be borne in mind. However, the growth of the CAF appears to begin quickly, and then decrease with time until there is a rapid change in insulation resistance as the final gap closes. Figure 31 shows data for CAF growth between via gaps of four different distances, the smaller gaps fail earliest calculated using this approach.

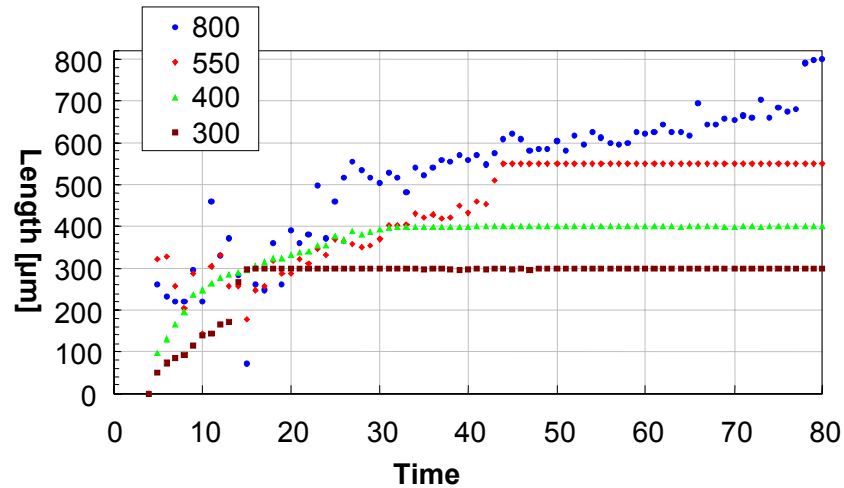


Figure 31. CAF growth extrapolated from IR time plot with resistive cylinder model (in-line, 5V, 0 cycles, 3 reflows)

4.1.6 Correlation of Phase 1 data to Sun/CALCE Models

Previous CAF studies from CALCE [8] and modifications by Sun Microsystems [16] have resulted in a proposed model for CAF growth. The adjusted CAF failure risk model is given as Equation 2.

Equation 2. CALCE/Sun Microsystems proposed CAF growth equation

$$t(F) = \frac{\rho \cdot a \cdot R \cdot T \cdot (L - 2 \cdot D)^2}{2 \cdot n \cdot F \cdot M \cdot C' \cdot H \cdot V} \cdot e^{E/R \cdot T}$$

Where:

- t(f) = time to failure
- D = distance from PTH to limit of "easily conductive region" surrounding PTH
- a = volume fraction of CAF in inter-electrode region
- L = initial interspace of the electrodes
- M = ion mobility constant (unknown)
- C' = copper ion concentration in a water solution
- F = Faraday constant (charge of one mole of electrons)
- N = number of valence electrons (n=2 for Cu²⁺)
- H = relative humidity
- E = activation energy
- V = voltage
- R = gas constant
- ρ = density of copper
- T = absolute temperature

If we group together parameters likely to be constant for a given laminate and test condition we can write:

Equation 3. Factors effecting CAF growth for given laminate and environmental conditions

$$t(F) \propto \frac{(L-2 \cdot D)^2}{V}$$

In order to fit the data collected in Phase 1 to this model the experimental data can be compared with a theoretical TTF based on the model. This is displayed in Figure 32, with experimental data calculated using Equation 3, a proportionality constant of 0.01, and a disrupted region (D) of 100 μ m.

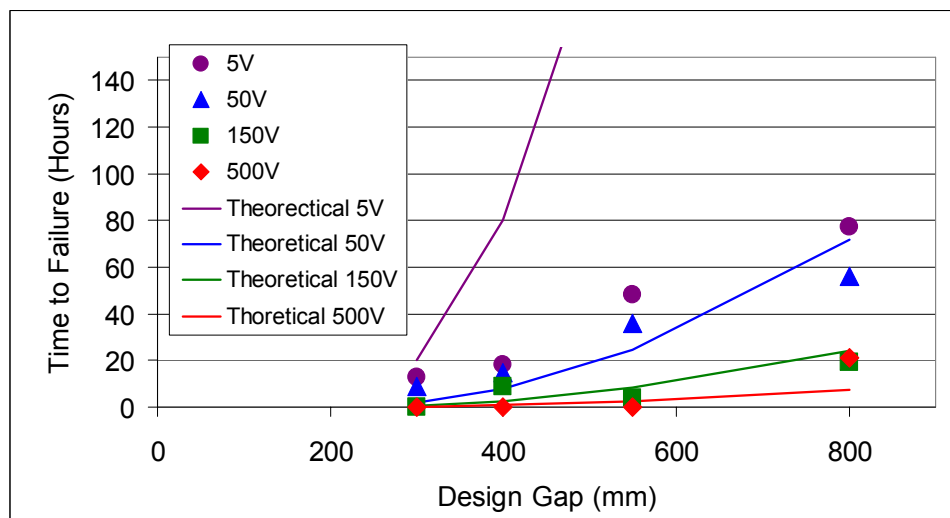


Figure 32. Experimental and theoretical data comparison, (in-line combs, no cycling, 3 LF reflows)

The design gap is the wall-to-wall gap predicted by the Gerber data for the board design. It can be seen that whilst we can select parameters to allow the model to predict TTF reasonably well with higher voltages, the model predicts failures times far in excess of those found experimentally with lower voltages. Adding the D term to the calculation improves agreement, but there still remains a poor fit to the data.

4.2 Phase 2

4.2.1 Normalisation of data for trend analysis

To maximise the value of the data, averages were taken across the entire matrix, selecting experiments where common parameters were available. This method would be the first step in a design of experiment approach that could not be considered here. Hence in order to study the effect of a particular parameter (for the example below ‘surface finish’) on CAF resistance the following procedure is applied.

1. Only data for samples in which **all other material and processing parameters were identical** were used in the calculation. This means the effects of processes other than the key variable (e.g. surface finish) did not influence trends.
2. For each style of comb pattern the time to failure (TTF) data are normalised against the average TTF for this subset. Equation 4 shows this calculation, where A_x is the normalised TTF for comb design A for condition (e.g. surface finish) x, TTF_{A_x} is the actual TTF for comb design A for condition x, and $TTF_{A_{mean}}$ is the mean TTF for comb design A across all conditions in the subset.

Equation 4. Normalisation of TTF data for a subset.

$$A_x = \frac{TTF_{A_x} - TTF_{A_{mean}}}{TTF_{A_{mean}}}$$

3. The normalised data are then averaged across all combs to give a mean normalised TTF for each condition.

4.2.2 Via geometry effects

4.2.2.1 Effect of via to via gap

Figure 33 shows the normalised TTF data across all the samples for different in-line comb geometries. Comparing the vertically aligned combs A to D the increase in via to via gap from 300 to 800µm results in an increase in TTF. The same trend is observed for the horizontally aligned combs E and G. These data back up the trends seen in Phase 1, i.e. larger via to via gaps are more resistive to CAF growth.

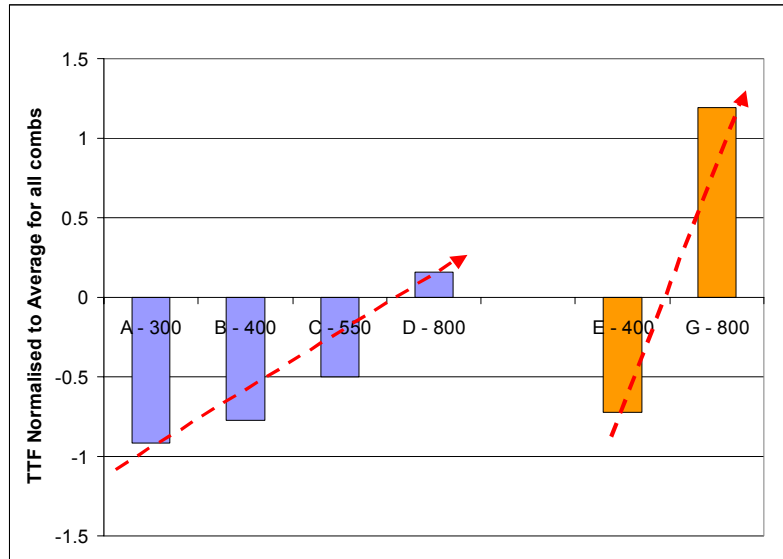


Figure 33. Effect of via wall-to-wall gap on TTF

4.2.2.2 Effect of layout

Figure 34 presents the normalised TTF data across all the samples in different comb orientations. The effect of weave can be seen with staggered vias being more resistant than those in-line, and horizontal combs being more resistant than vertical. This, again, supports the findings of the Phase 1 work, with the improvement in CAF resistance for staggered combs coming from the lack of direct glass fibre contact between the two via walls. The properties of the warp and weft fibres are clearly different for the 800μm data.

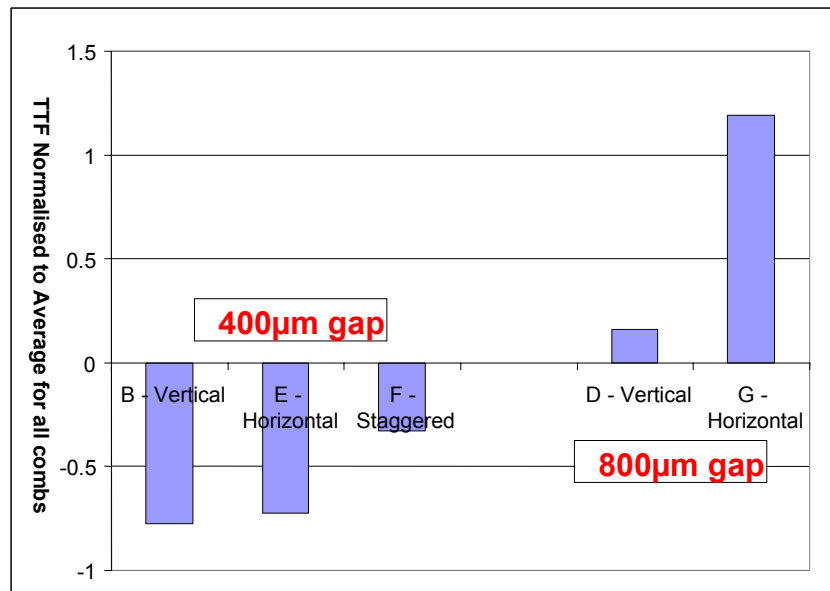


Figure 34. Effect of via alignment to glass weave on TTF, for 2113 and 2116 laminates

4.2.2.3 Effect of inner layer pads and polarity

The normalised TFF data for the anti-pad combs (see Figure 35), do not centre around zero because the analysis was performed for all the combs, but only the data for the anti-pad combs (with generally longer TTF) are plotted. It is clear that if the via is the anode (positive bias) then the CAF resistance of the system is dramatically reduced compared to the reverse polarity system. The CAF grows much quicker from a via anode initiation site than from a copper plane anode, consistent with the damaging effect drilling is thought to cause.

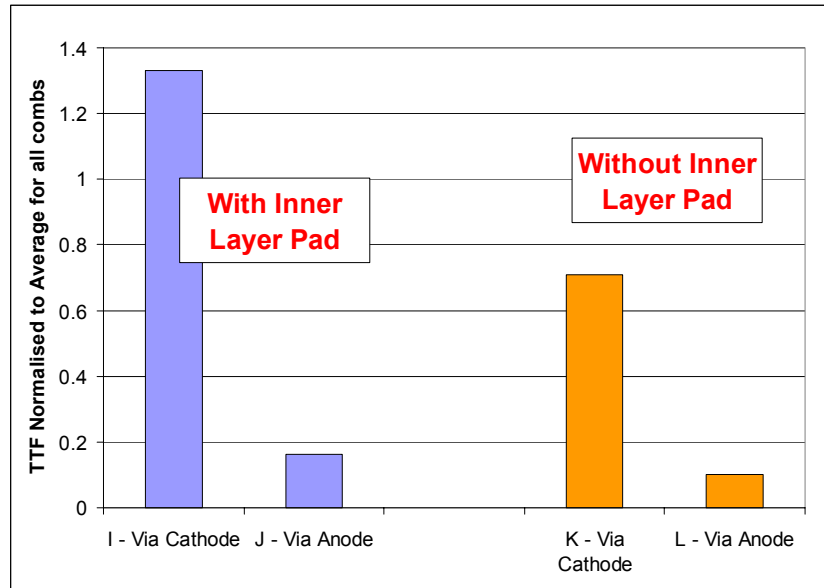


Figure 35. Effect of inner layer pads and via polarity

Moreover, there appears to be no significant change in CAF performance as a result of the presence of inner layer pads for CAF growing from the via wall (Combs J and L). This lends support to the conclusions in Phase 1 (Section 4.1.2.3) that the CAF grows from the via wall (associated with the ends of the glass fibres) and not the edge of the inner layer pad (held in between the reinforced pre-preg layers away from the fibres).

For the case where CAF grows from the copper planes (combs L and J) the failures are earlier for the configuration with inner layer pads (J). This is because the effective distance for the CAF to grow is reduced by the presence of the pad (see Figure 36).

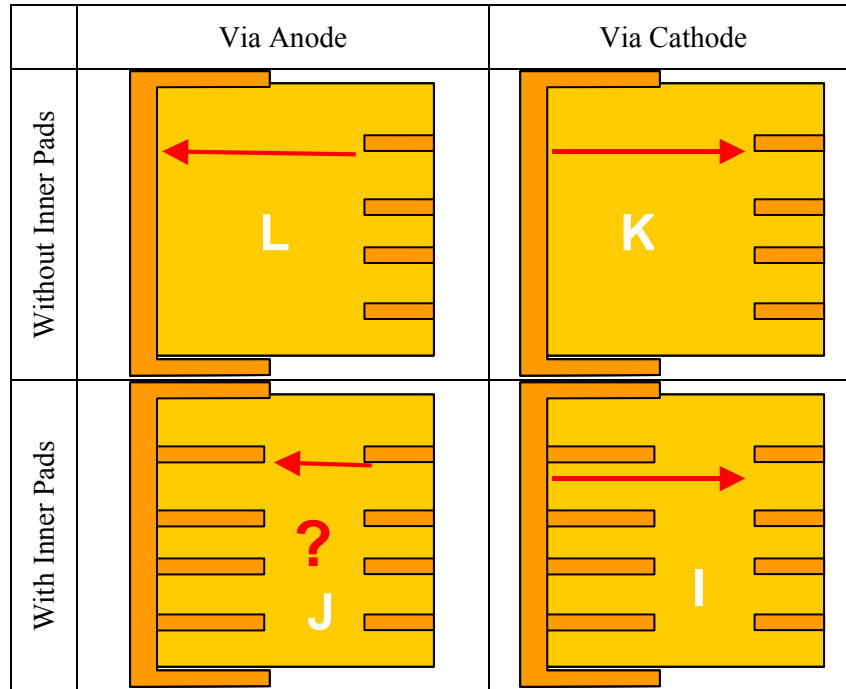


Figure 36. The effective distances for CAF growth in anti-pad configurations

4.2.3 Process and material effects

In this Section the following nomenclature system was sometimes used to label plots to identify materials:

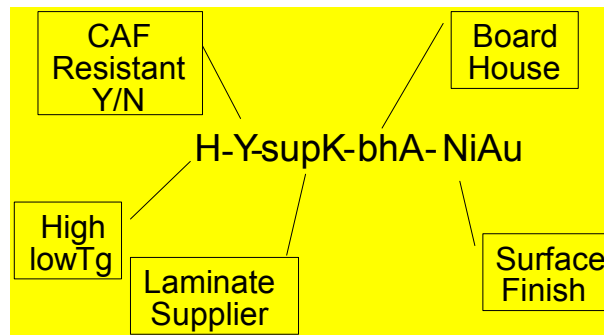


Figure 37. Labelling format for 'process and materials effect' plots.

In many cases parameters were the same for all the materials tested to aid direct comparison, in which case the parameter was included in the code but was also included in the caption for the plot.

4.2.3.1 Effect of PWB surface finish

There are potentially a large number of chemical processes used in the application of surface finish chemistries in board production. Since the CAF mechanism involves the migration of ions and the formation of copper salts it is possible these residues may impact on CAF formation. In order to investigate any possible trends in CAF resistance caused by the use of

different printed circuit solderable finishes the data from a variety of samples (processed as in Table 4) were compared.

Table 4. Conditions for coupons selected for comparison of the effects of surface finish

Board House:	B
Drill Feed Speed:	1 (standard feed)
Reinforcement:	2116-type
Reflow Profiling:	3 lead-free exposures
Laminate Supplier:	K
Laminate Tg:	High
Laminate CAF Designation:	Yes, No
Surface Finish:	NiAu, Ag, HASL, OSP

The normalised TTF data are plotted in Figure 38. There were two different materials included: one CAF resistant and one non-CAF resistant. The effect of different surface finishes did not appear significant for the non-CAF resistant material. The standard deviation of the mean was plotted as an error bar, and shows the low significance of the differences. The normalised TTF for the silver finish is high for the CAF resistant laminate, but not so for H-N-supK ‘DICY’ cured laminate with Ag finish (although deviation in the longer TTF values is high). It is not clear why the silver finish provided good results for H-Y-supK laminate.

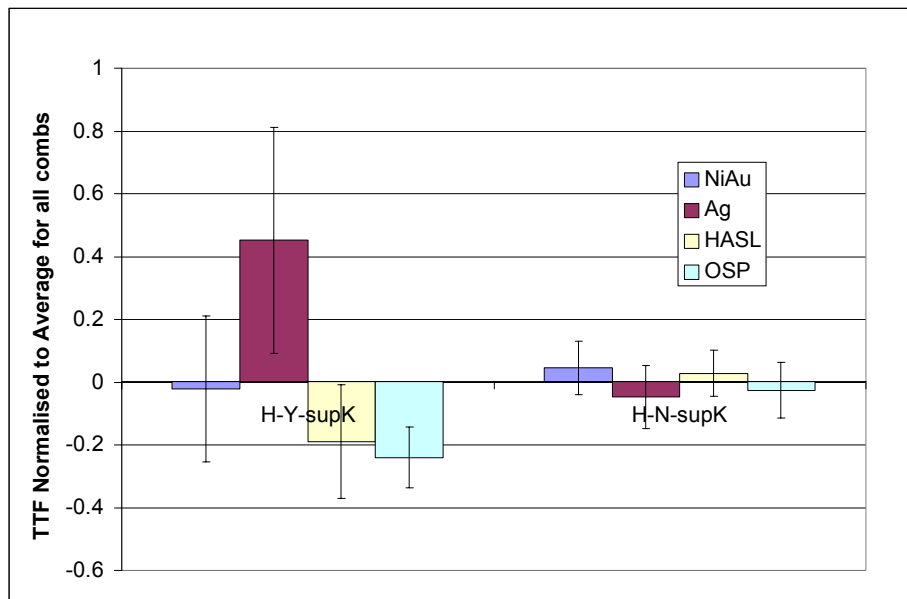


Figure 38. Effect of surface finish on TTF

4.2.3.2 Effect of drill feed speed

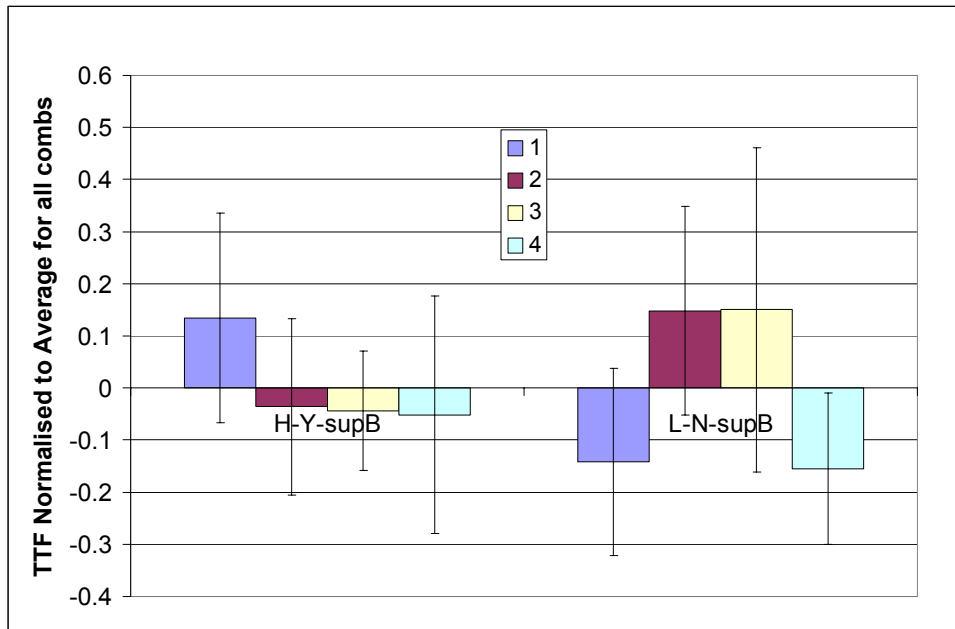
During drilling the drill bit is driven into the laminate at a controlled feed rate (Note: This is not the speed at which the drill spins). Faster feed speeds mean quicker production, however it has been postulated that forcing high feed speeds results in more damage to glass fibres during drilling, which in turn could provide a greater number of initiation sites for filaments.

In order to investigate any possible trends in CAF resistance caused by the use of different printed circuit drill speeds the data from a variety of samples (processed as in Table 5) were compared.

Table 5. Conditions for coupons selected for comparison of the effects of drill feed speed

Board House:	C
Drill Feed Speed:	1, 2, 3, 4
Reinforcement:	2116
Reflow Profiling:	3 lead-free exposures
Laminate Supplier:	L
Laminate Tg:	High, Low
Laminate CAF Designation:	Yes, No
Board Finish:	NiAu

Figure 39 presents the normalised TTF data for the different drill speeds, and it seems that there is no significant effect of drill feed speed for the laminates and processing conditions used in this study.

**Figure 39. Effect of drill speed.**

Sectioning of the samples did not uncover any significant difference in the quality of the drill hole (i.e. copper plating ingress into glass fibre bundles). Despite the higher feed rates the drill hole quality appeared to still be acceptable, resulting in little difference between the samples tested. Perhaps the use of blunt or overused drills would give a greater differentiation in drill hole quality.

4.2.3.3 Effect of reflow conditions

The Phase 1 study results (Section 4.1.2) indicated that it was the high peak reflow temperature that reduced CAF performance, not thermal shock. This suggests that the mechanism for damage in the laminate is not based on TCE mismatch between the materials in the composite FR4, but perhaps a chemical or physical breakdown at a certain temperature. An investigation of reflow conditions was therefore included in Phase 2, using the samples processing in line with Table 6.

Table 6. Conditions for coupons selected for comparison of the effects of reflow conditions

Board House:	A
Drill Feed Speed:	1
Reinforcement:	2116
Reflow Profiling:	None, 3L, 3LF
Laminate Supplier:	K, L, M
Laminate Tg:	High, Low
Laminate CAF Designation:	Yes, No
Board Finish:	NiAu

In Figure 40 the normalised TTF data are plotted for five laminate types exposed to different reflow conditions. A significant trend to lower CAF performance after increasing exposure to lead-free reflow conditions, compared to tin-lead reflow exposure, can be seen. Whilst the reflow conditions used can be considered “worst case” this could be a concern for those manufacturing high reliability multi-layer product, especially with high via densities as they switch to lead-free production.

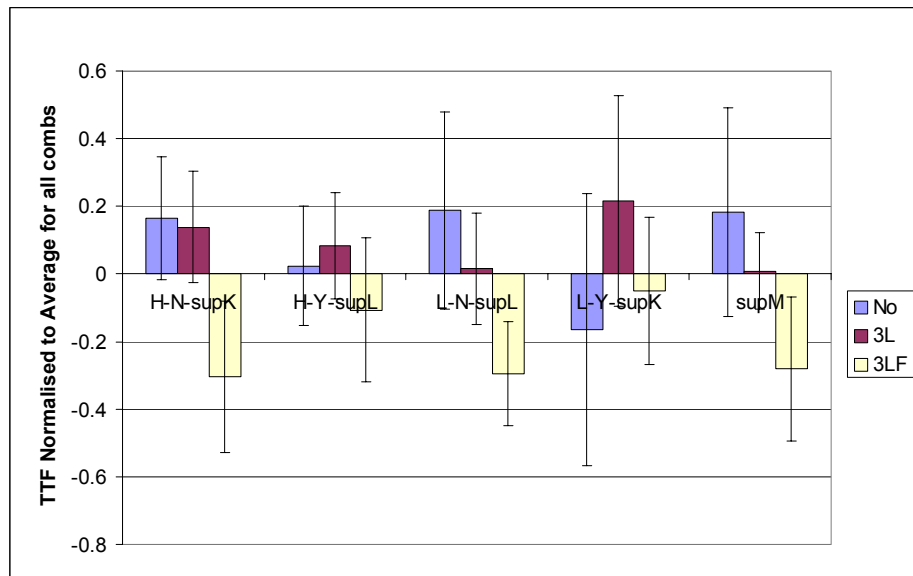


Figure 40. Effect of reflow exposure

4.2.3.4 Effect of printed circuit manufacturing location

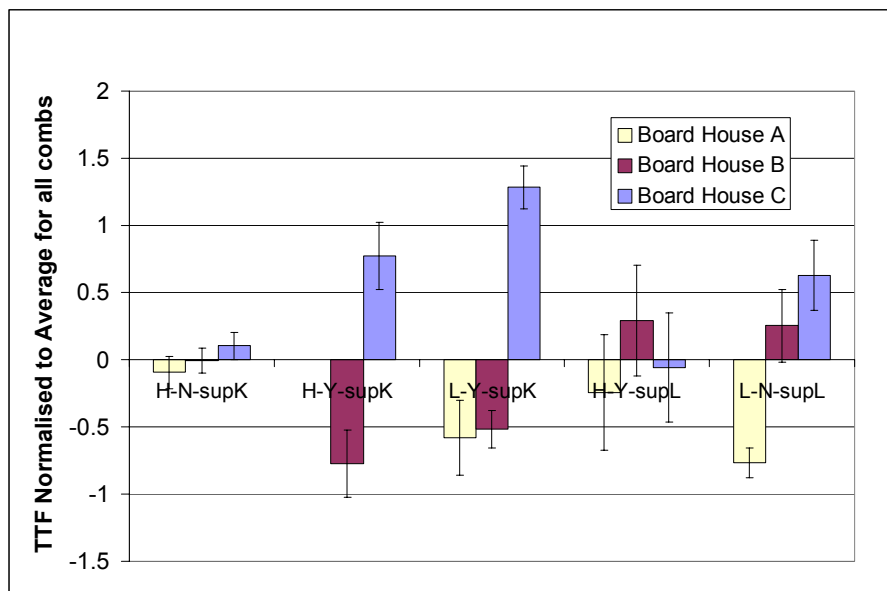
The number of processes and parameters involved in the manufacture of printed boards is immense. Some have been specifically investigated as part of this work, but there are many others that have not. Examples include lamination press cycle (temperature, pressure, time), alignment accuracy, and copper seeding and plating processes. For these processes the production partners were asked to use their standard production conditions for this type of board.

To establish whether there were any differences in product from different board houses produced under “house” conditions, identical board samples were processed at three locations as shown in Table 7.

Table 7. Conditions for coupons selected for comparison of the effects of board house

Board House:	A, B, C
Drill Feed Speed:	1 (standard)
Reinforcement:	2116- type
Reflow Profiling:	3LF
Laminate Supplier:	K, L
Laminate T _g :	High, Low
Laminate CAF Designation:	Yes, No
Board Finish:	NiAu

The normalised TTF data showing the effect of manufacturing location on the CAF performance of five laminate types are shown in Figure 41. Clearly the effect of where the laminate is manufactured has significant impact on CAF. It can be seen that generally for materials manufactured at board house C, boards are more CAF resistant, and those produced at board house A were the least CAF resistant. This is a surprising result and the cause of this is not understood by the project group, and could be an effect of one of many processes taking place during the laminate build-up.

**Figure 41. Effect of manufacturing location (board house)**

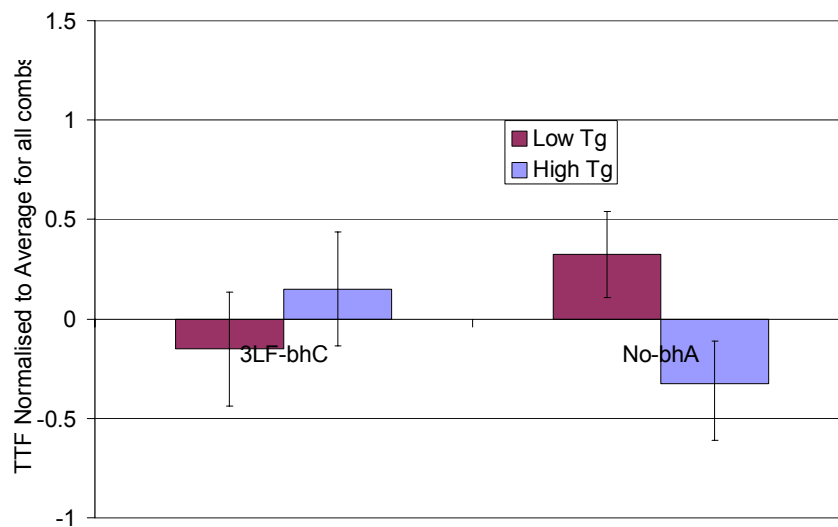
4.2.3.5 Effect of material T_g

The epoxy formulation for FR4 is often available as standard T_g or high T_g (Section 3.3.3). High T_g material is often specified for high temperature applications, although its resistance to thermal degradation is no better than standard laminate. In order to see if the T_g of the laminate epoxy used had any effect on CAF performance the samples in Table 8 were analysed.

Table 8. Conditions for coupons selected for comparison of the effects of laminate T_g

Board House:	A, C
Drill Feed Speed:	1 (standard)
Reinforcement:	2116-type
Reflow Profiling:	No, 3LF
Laminate Supplier:	K
Laminate T _g :	High, Low
Laminate CAF Designation:	Yes
Board Finish:	NiAu

In Figure 42 normalised TTF data showing the effect of T_g are given. No clear effect of T_g is apparent for the laminates tested here, and it is not possible to make any recommendation regarding T_g.

**Figure 42. Effect of material glass transition temperature**

4.2.3.6 Effect of glass reinforcement

The effect of different styles of glass fibre-reinforcement was investigated using the samples listed in Table 9.

Table 9. Conditions for coupons selected for comparison of the effects of glass reinforcement

Board House:	B
Drill Feed Speed:	1 (standard)
Reinforcement:	2116, 2113-type
Reflow Profiling:	3LF
Laminate Supplier:	K, L
Laminate T _g :	High, Low
Laminate CAF Designation:	No
Board Finish:	NiAu

The normalised TTF data for the two laminate types are shown in Figure 43. For the K laminate the effect of the glass fibre reinforcement seems to have a negligible effect, but for the laminate from supplier L the difference is significant with the 2116 weave providing

greater CAF resistance. These ambiguous results mean that under certain circumstances the weave may well be an issue and one that deserves further study.

Note: The data in Figure 43 are normalised to show differences due to weave, and so the longer failure times for horizontal combs were not revealed. As such this is not in conflict with Figure 34 or comments in Section 4.2.2.2.

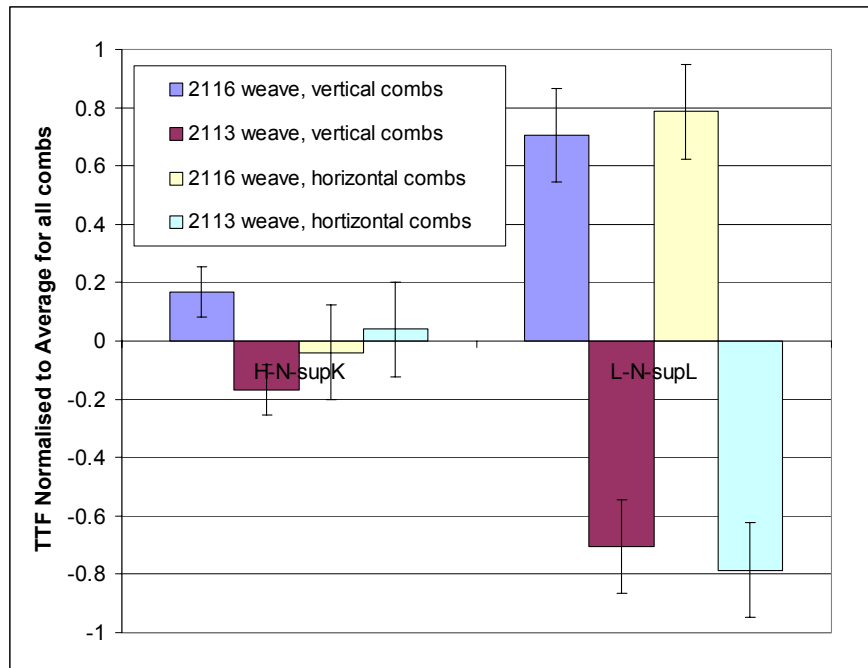


Figure 43. Effect of glass reinforcement on TTF

4.2.3.7 Effect of laminate CAF chemistry

The effect of chemistry in the epoxy make-up (CAF, or non-CAF resistant) was investigated using the samples listed in Table 10.

Table 10. Conditions for coupons selected for comparison of the effects of CAF designation

Board House:	A, B, C
Drill Feed Speed:	1 (standard)
Reinforcement:	2116, 1080-type
Reflow Profiling:	3LF
Laminate Supplier:	K
Laminate Tg:	High
Laminate CAF Designation:	Yes, No
Board Finish:	NiAu, HASL, OSP, Ag

The normalised TTF data for the six different laminate types are shown in Figure 44, covering a broad range of process conditions and materials. *In all cases it can be seen that the use of a laminate formulated for 'CAF resistance' does indeed provide an increased resistance to the onset of CAF. It does not eliminate it, however, under high stress conditions.*

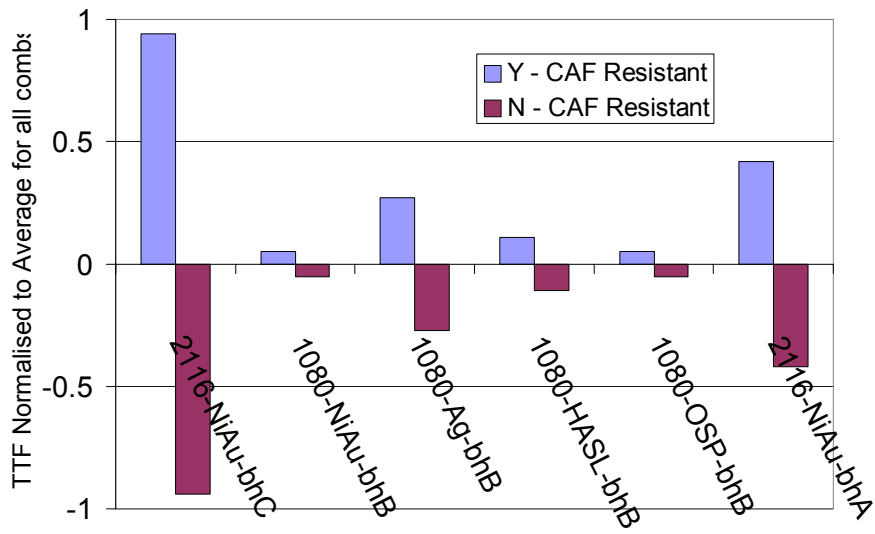


Figure 44. Effect of CAF chemistry on TTF

5 DISCUSSION

The test method developed in this study has been successful in measuring the susceptibility of glass-reinforced epoxy laminates to CAF failures. Microsectioning, polishing and EDAX analysis results have confirmed the presence of CAF in test pieces. The presence of Cl, S, Ni, Zn as well as copper are associated with the filament suggesting chemical residues from many processes or materials can be involved in the electrochemical filament formation (e.g. nickel from ENIG process, sulphur from plating baths, zinc from seeding chemistry, chlorine from acid etch).

It has been demonstrated that CAF can be detected by measurement of changes in electrical resistance between through hole via walls, or at other failure sites within the test vehicle. When CAF bridges a gap between two conductors the loss of electrical insulation is rapid.

The method allows a comparison of material and processing parameters, showing the relative beneficial or harmful effects on product reliability in terms of potential CAF failures. It has been shown clearly that a main concern for those designing and manufacturing electronic laminates must be the significantly earlier failures promoted by decreasing geometries in multilayer board designs. For electronics companies looking at technology roadmaps this may be an important limiting factor, especially for those with space/weight sensitive applications, or humid and aggressive end use environments, as illustrated in Figure 45.

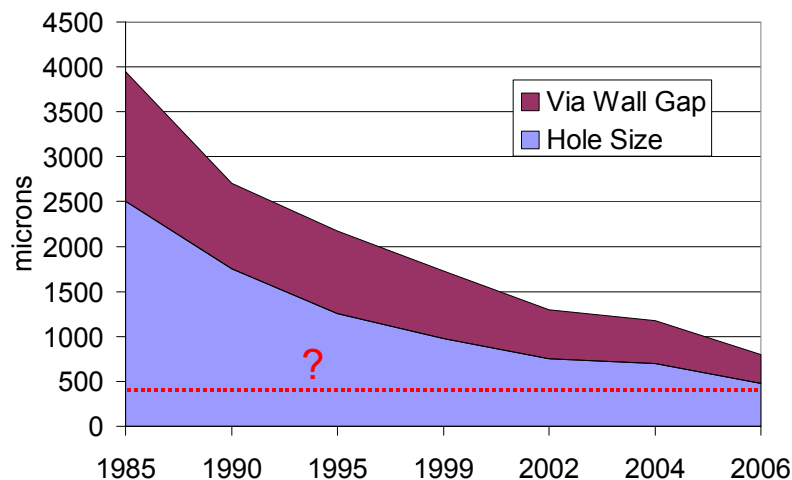


Figure 45. CAF could be a roadblock for size reduction in technology roadmaps [5]

By July 2006 electronics manufactured in the EU must be made with lead-free solder, meaning an increase (commonly around 30°C) in peak soldering temperature as a result of replacement eutectic alloys. Data suggest that the high peak temperatures seen in reflow operations have a detrimental effect on laminate reliability, and so lead-free introduction will have an impact. Whilst laminates can visually darken (when uncovered by solder mask) due to overheating, previous research suggests that the insulation between surface PCB features remains unaffected in lead-free processes [6], see Figure 46. Clearly it is important that the same assumption for sub-surface failures in multilayer boards is not made, as the risk of CAF initiation and growth will increase.

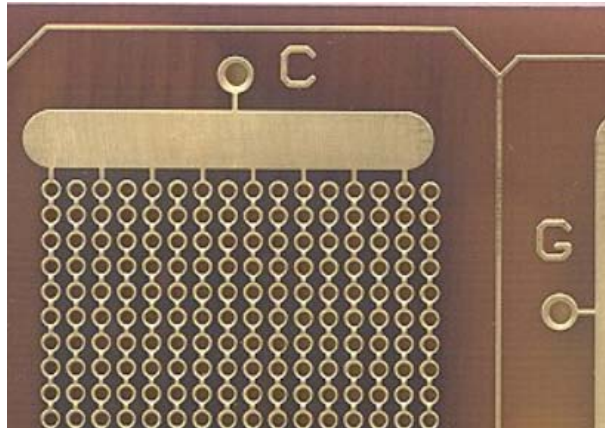


Figure 46. Epoxy laminates can darken in lead-free reflow, but potential problems could be below the surface

One of the most interesting findings of this research is that the manufacturing undertaken by the board house (etching, permanganate desmear, seeding, plating, board lay-up, bonding/press cycles, etc) has a significant impact of the resultant resistance to CAF. *Whilst the scope of this study did not cover an investigation of these individual processes it is clear that specifying materials alone is not adequate, and for better product quality board house processing needs to be understood and controlled. There is certainly potential for further work in this area.*

The trends seen in the accelerated tests support the assertion that CAF always grows from an anodic conductor and preferentially from copper associated with a via wall. CAF can grow from other initiation sites, such as copper planes, but times to failure are much longer. These findings fit well with the mechanism for CAF proposed in Section 2.

Damage of the glass reinforcement fibres during drilling is thought to be a cause of 'copper spears' radiating from the plated via walls, concentrating the electric field and becoming initiation sites for CAF growth. Whilst no significant dependence on drill feed speed was observed in this work, micro-sections demonstrated that the wall quality was good for all the samples. It may be that drill rotation speed and drill quality are more critical in affecting glass damage and subsequent copper ingress, than is the feed speed for drilling. From Figure 47 it can be seen there are no significant points of copper ingress out from the plated via wall, and this was typical of all samples sectioned across a range of materials. As such this study suggests that drill hole quality can be good even with high feed rates, but does not suggest that hole quality has no effect on CAF susceptibility. It is also evident that with high quality holes CAF will still occur under high stress conditions.

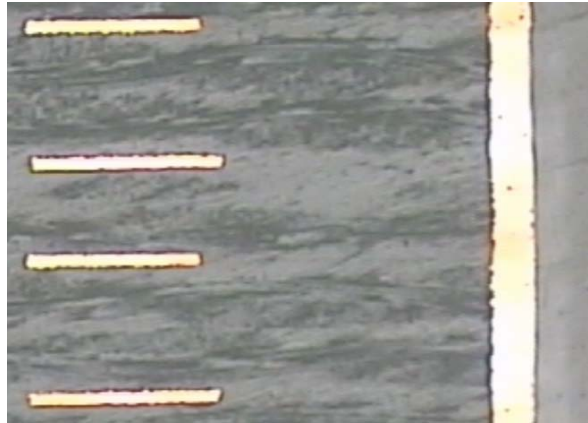


Figure 47. Drilled wall quality was very good for all samples.

There are choices that can be made which can increase product CAF reliability. Design choices include keeping via walls well spaced, and if possible staggering those that are close at 45° to the glass weave. By choosing ‘DICY’ free, or CAF resistant laminate from the supplier the risks of CAF can be much reduced, but higher Tg materials are not necessarily more resistant to CAF than those with a lower Tg.

The effects are summarised in Figure 48 where the differences in normalised time to failure as the result of changes in process and material are shown.

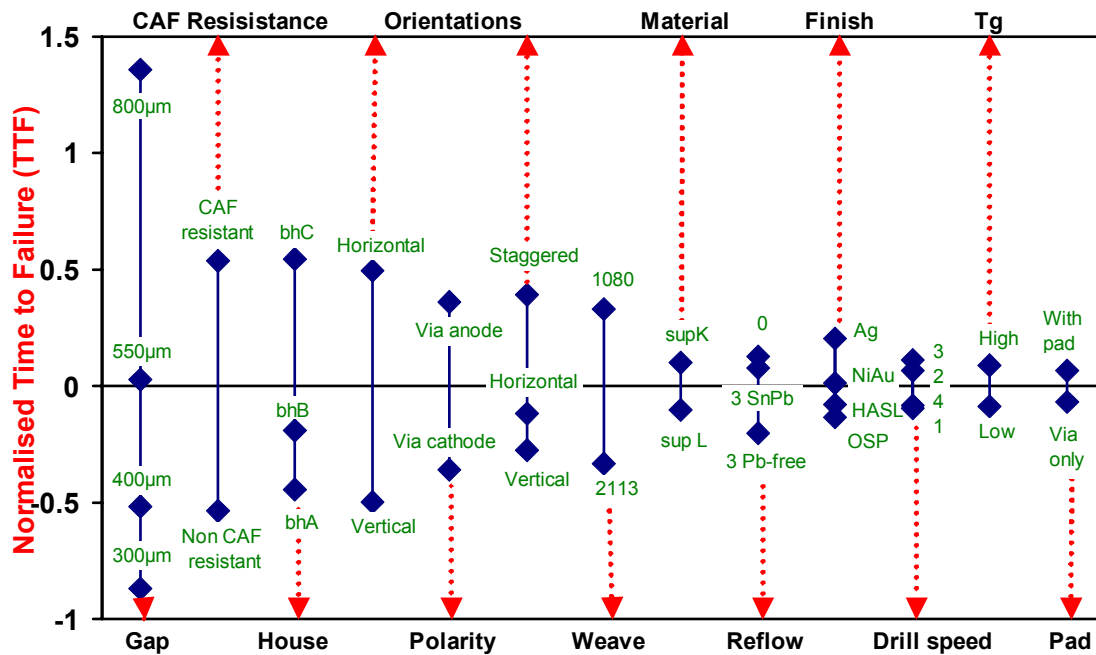


Figure 48. Normalised plot showing effects of material and process on CAF time to failure

6 CONCLUSIONS

The test method used in this study has proved to be sensitive for monitoring changes in CAF resistance for laminates. The fundamentals of the technique are:

- A multi-layer glass-reinforced epoxy laminate test vehicle
- Manufacture and processing of the laminates using actual conditions for product
- Insulation resistance combs incorporating drilled and plated vias in proximity representing a range of geometries
- Application of a DC voltage across vias to provide a driving force for CAF growth
- High temperature and humidity exposure (85°C, 85%RH) for up to 1000 hours
- Frequent monitoring of insulation resistance to determine the time to failure for each test comb

The following parameters have been found to have a significant effect upon CAF resistance:

- Design geometries
 - Via to via gap
 - Vias closer together are more susceptible to CAF, even at the same voltage gradient
 - Via and ground planes
 - Anodic vias fail faster than geometrically identical cathodic vias
 - Inner Layer Pads
 - CAF resistance is reduced for geometries where CAF growth is initiated from copper plane, which has an intrinsically higher resistance
- Alignment to reinforcement
 - Warp and weft directions can show markedly different resistances to CAF, both must be examined
 - Via staggered at 45° to the lay-up have a resistance to CAF greater than those aligned with warp or weft with the same gap
- Voltages
 - Higher voltages decrease the time to failure for the same geometries (i.e. reduce CAF resistance)
- Laminate system
 - 'CAF resistant' (DICY free) resins reduce the risk of CAF formation
 - Identically specified laminates from different suppliers can have different CAF performances
- Reflow conditions
 - Peak temperatures of 250°C in reflow are potentially harmful to the CAF performance of the laminate
- Manufacturing
 - The in-house processing of laminate at board houses results in laminates with different CAF performances

The following parameters had a much less significant effect on CAF performance:

- Boards solderability surface finish
- Drill feed rate during via drilling
- Presence or size of inner layer pads
- High/low T_g designation of laminate
- Thermal Shock of laminate

It is important for end users wishing to qualify product, to recognise that laminate must be tested as manufactured by the board house, and that it may not be sufficient just to specify CAF resistant laminate (although this improves things) since other parameters have effects of the same order of magnitude.

7 REFERENCES

- [1] LANDO, D., MITCHELL, J.P., WELSHER T.L., Conductive anodic filaments in reinforced polymeric dielectrics: formation and prevention. *Proc. 17th Annual Reliability Physics Symposium.*, April 1979, pp 51 - 63.
- [2] READY, W.J., STOCK, S.R., FREEMAN, G.B. DOLLAR, L.L., TURBINI, L.J. Microstructure of conductive anodic filaments formed during accelerated testing of printed wiring boards. *Circuit World*, 1995, **Vol. 21, No.4**, pp5 -9.
- [3] HUNT, C.P. Development of surface insulation resistance measurements for electronic assemblies. *NPL Report MATC(A)70*, October 2001.
- [4] WICKHAM, M. 'Thermal profiling of electronic assemblies'. *NPL Report MATC(A)50*, September 2001
- [5] Adapted from Sun Microsystems roadmap: Report of the IPC Standards Development Activities, Electrochemical Migration Task Group, 5-32e, *Report of Task Group – Sept00*.
- [6] WICKHAM , M., ZOU, L., HUNT, C. 'An assessment of the suitability of current pcb laminates to withstand lead-free reflow profiles'. *NPL Report MATC(A)91*, April 2002
- [7] RUDRA, B. Electrochemical migration in multichip modules. *Surface Mount International Conference and Exposition*. Edina, MN, USA, 1994, Proceedings of the Technical Program, NY, USA: Surface Mount Int, IPC, 1994. p.50-6
- [8] BI-CHU WU, PECHT, M., JENNINGS, D. Conductive filament formation in printed wiring boards. *Thirteenth IEEE / CHMT International Electronics Manufacturing Technology Symposium*. Edina, MN, USA, 1994, IEEE, 1992, p.74-9
- [9] TSUJIOKA, N., PECHT, M., JENNINGS, D. Generative mechanisms and preventive methods for micro-defects in PCB. *Proceedings of the Printed Circuit World Convention*, Aylesbury, UK, 1990, Hazell Books, 1990, pB2 / 3-12
- [10] MITCHELL, J.P., WELSHER, T.L. Conductive anodic filament growth in printed circuit materials. *Proceedings of the Printed Circuit World Convention II*, Wurtz, Germany, Eugen G. Leuze Verlag, 1981, p.80-93 vol.1 of 2 vol.
- [11] WELSHER, T.L., MITCHELL, J.P., LANDO, D.J. Conductive anodic filaments (CAF): an electrochemical failure mechanism of reinforced polymeric dielectrics, *1980 Annual Report. Conference on Electrical Insulation and Dielectric Phenomena*, Washington, DC, USA, 1980, Nat. Acad. Press, Acad. Press, 1980. p.234-9
- [12] WELSHER, T.L., MITCHELL, J.P., LANDO, D.J. CAF in composite printed-circuit substrates: characterization, modelling and a resistant material., *18th Annual Proceedings of Reliability Physics New York*, NY, USA, IEEE,1980. p.235-7
- [13] SHUKLA, A., PECHT, M., JORDAN, J., ROGERS, K. , JENNINGS, D. Hollow fibres in PCB, MCM-L and PBGA laminates may induce reliability degradation. *Circuit World*. Jan 1997, **Vol.23**, No.2, p. 5-6

- [14] SHUKLA, A.A.; DISHONGH, T.J.; PECHT, M.; JENNINGS, D. Hollow fibres in woven laminates [packaging reliability]. *Printed Circuit Fabrication*. Jan 1997, **Vol.20**, No.1, p. 30-2
- [15] RUDRA, B.; JENNINGS, D. Failure-mechanism models for conductive-filament formation. *IEEE Transactions on Reliability*. Sept 1994, **Vol.43**, No.3, p. 354-60
- [16] SAUTER, C. IPC Users Guide for Electrochemical Migration Conductive Anodic Filament (CAF) Testing. Developed by Electrochemical Migration Task Group (5-32e) of the Cleaning and Coating Committee (5-30). Due for release 2004, at the time of writing.

8 ACKNOWLEDGEMENTS

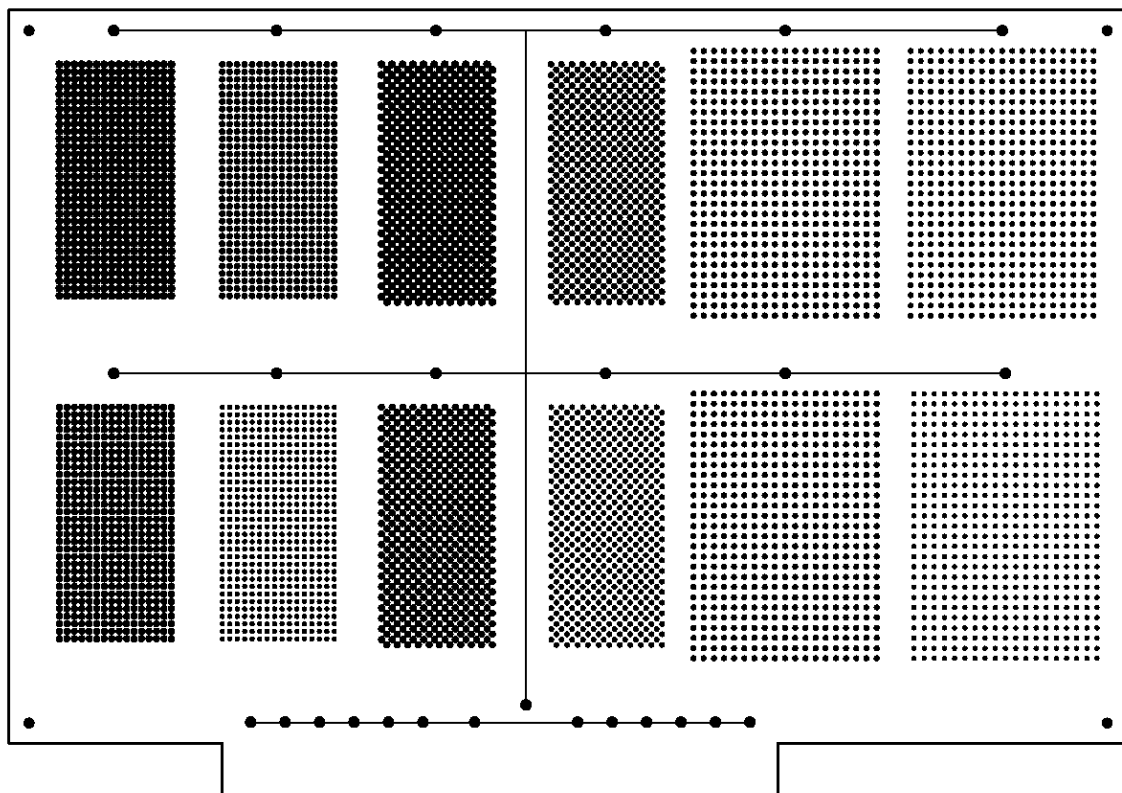
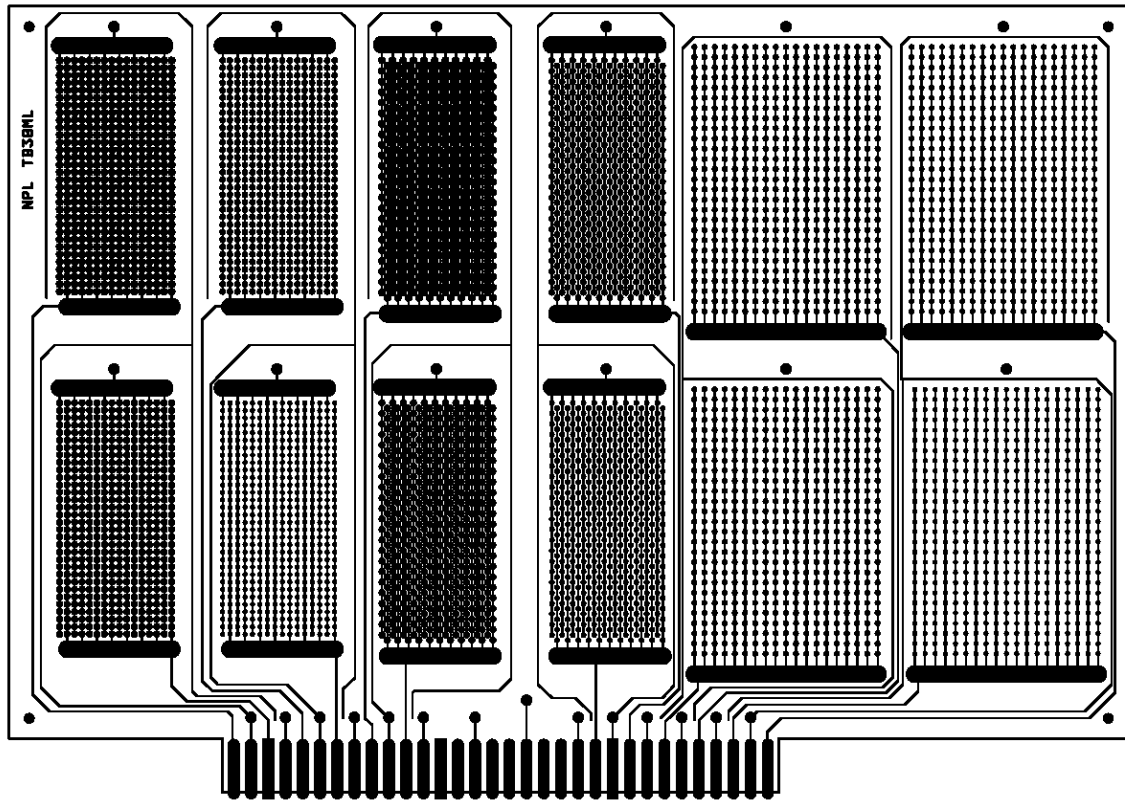
The work was carried out as part of the Studio Programme within the Materials Processing Metrology Programme of the UK Department of Trade and Industry. The authors would like to thank the industrial partners for their supporting their project and for their time, intellectual property and manufacturing assistance. The partners were:

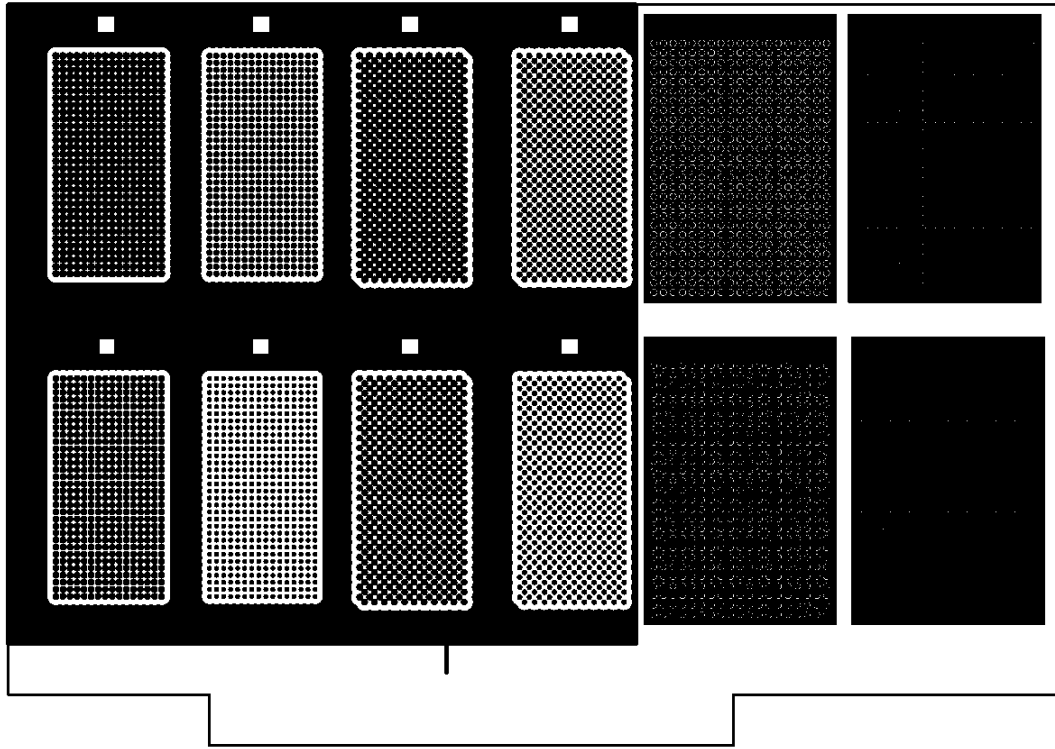
Alcatel Submarine Networks
Graphic Plc
Invotec
Isola
PolyClad
Prestwick Circuits
TRW Automotive
Concoat Ltd

The authors would like to acknowledge the assistance of Milos Dusek at NPL with the design and production of Gerber files.

9 APPENDIX A – GERBER PLOTS FOR TB38A

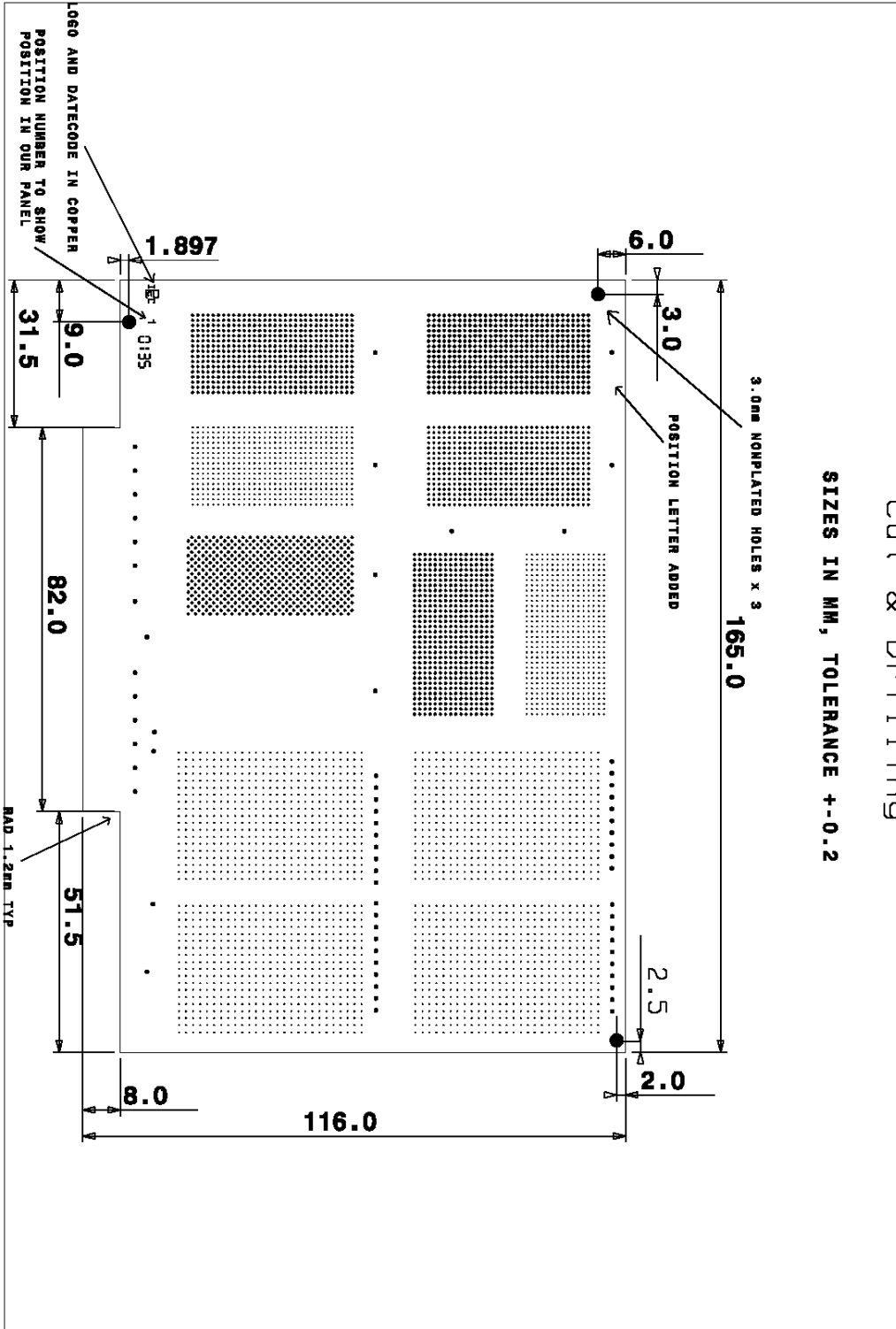
Files available upon request, www.npl.co.uk/ei



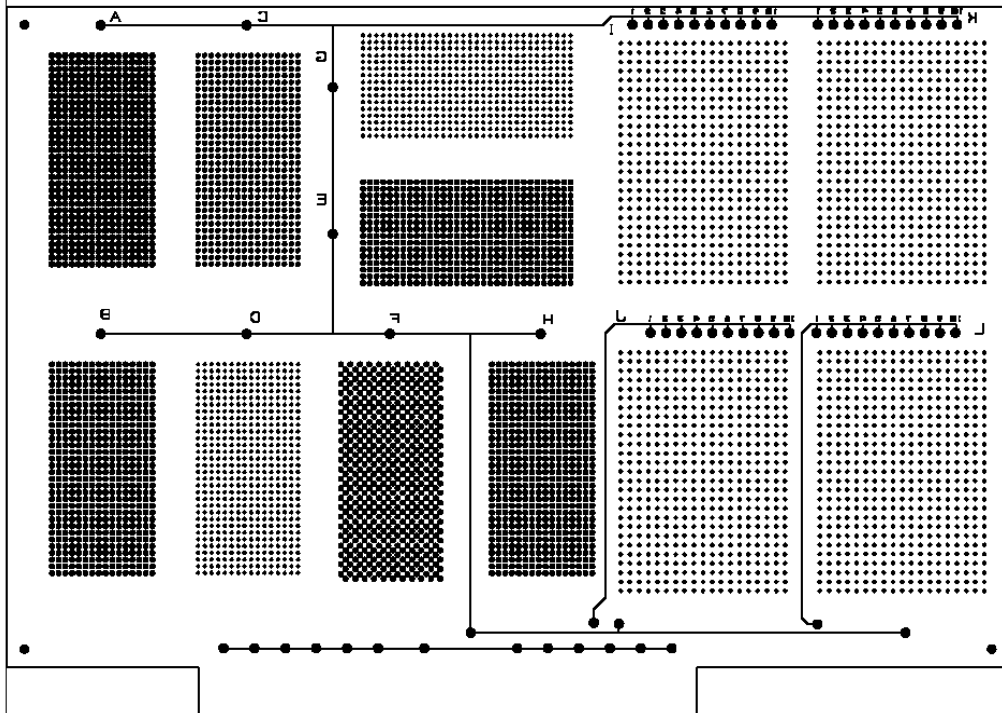


10 APPENDIX B – GERBER PLOTS FOR TB38B

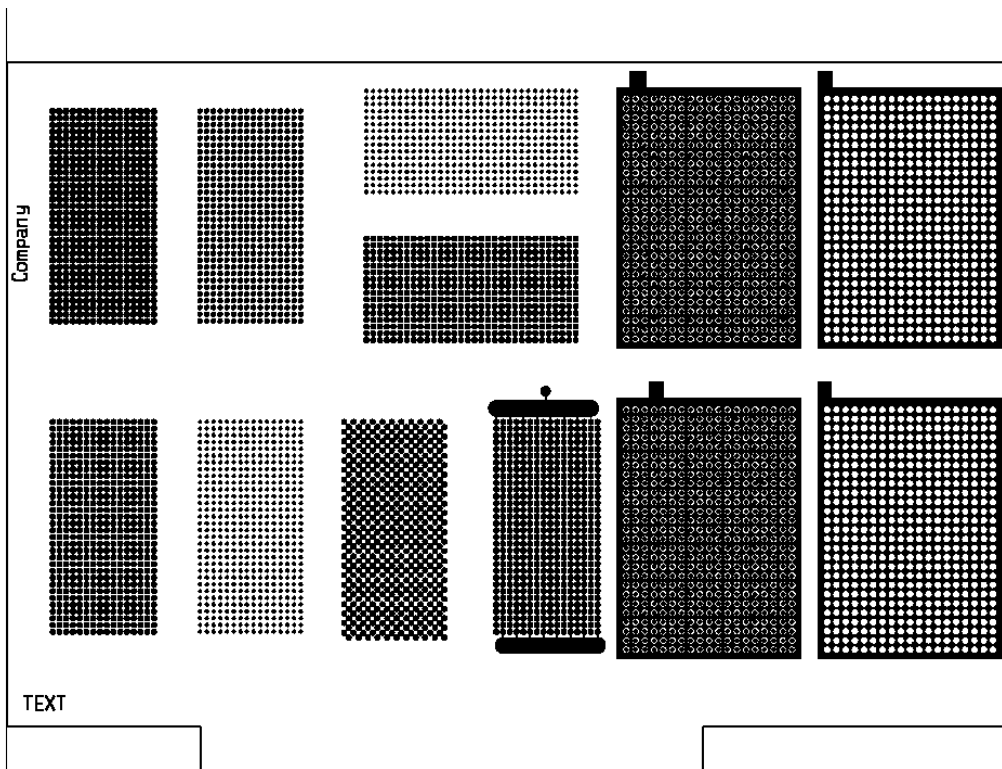
Files available upon request, www.npl.co.uk/ei



Bottom Cu

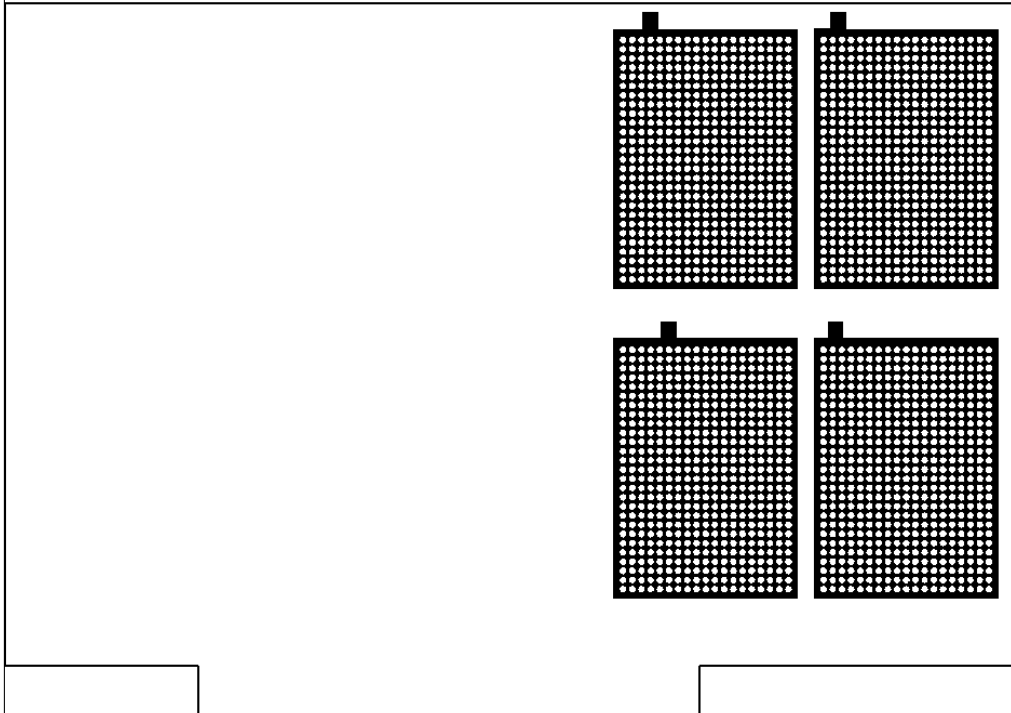


TB38B.GTD, 04:33 PM, 02/05/02, OrCAD



TB38D.GTD, 01:22 PM, 02/06/02, OrCAD Gerber

Inner 2(B)



TB38B.GTD, 04:41 PM, 02/05/02, OrCAD Gerb